Quantum percolation and ballistic conductance on a lattice of wires

Y. Avishai
Service de Physique Théorique, CE Saclay, F91191 Gif-sur-Yvette, CEDEX, France
and Department of Physics, Ben Gurion University, Beer Sheva, Israel

J. M. Luck
Service de Physique Théorique, CE Saclay, F91191 Gif-sur-Yvette, CEDEX, France
(Received 18 June 1991)

Motivated by concepts of classical electrical percolation theory, we study the quantum-mechanical electrical conductance of a lattice of wires as a function of the bond-occupation probability p. In the ordered or ballistic case ($p=1$), we obtain an analytic expression for the energy dispersion relation of the Bloch electrons, which couples all the transverse momenta. We also get closed-form expressions for the conductance g_{NL} of a finite system of transverse dimension N^{d-1} and length L (with $d=2$ or 3). In the limit $L\to\infty$, the conductance is quantized similarly to what is found for the conductance of narrow constrictions. We also obtain a closed-form expression for the conductance of a Bethe lattice of wires and find that it has a band whose width shrinks as the coordination number increases. In the disordered case ($p<1$), we find, in $d=3$ dimensions, a percolation transition at a quantum-mechanical threshold p_q that is energy dependent but is always larger than the classical percolation threshold p_c. Near p_q (namely, for small values of $|\Delta|\equiv|p-p_q|$), the mean quantum-mechanical conductance $\langle g_L\rangle$ of a cube of length L follows the finite-size-scaling form $\langle g_L(p)\rangle\approx L^{d-2-t/\nu}F(\Delta L^{1/\nu})$, where the scaling function F and the critical exponent ν are different from their classical analogues. Our numerical estimate of the critical exponents is $\nu=0.75\pm0.1$ and $t=\nu$ in accordance with results of nonlinear σ models of localization. The distribution of the conductance undergoes a substantial change at threshold. The conductance in the diffusive (metallic) regime in $d=3$ dimensions follows Ohm's law (it is proportional to L). As $p\to1$, the crossover between the metallic and the ballistic regimes is governed by the scaling law $\langle g_L(p)\rangle\approx L^2K(L(1-p))$. No percolation transition is found for $d=2$ but as $p\to1$, the crossover between the quasimetallic and the ballistic regimes is governed by a similar scaling law.

I. INTRODUCTION

This work is devoted to the study of wave propagation through binary inhomogeneous media. Specifically, we intend to investigate quantum-mechanical transmission through a binary lattice of quantum wires. This study will naturally cover various transport phenomena due to the intimate relation between transmission and quantum-mechanical dc electrical conductance at zero temperature. Our investigation will cover also wave propagation and Bloch states of ordered systems such as a regular lattice of wires (for which the energy-dispersion relation and transmission coefficients are computed analytically) and a Bethe lattice.

Guided by classical analogs, we model quantum-mechanical transport properties of binary composite media by considering a (d-dimensional) regular lattice consisting of sites and links (also referred to as bonds). These links are treated as very narrow waveguides (quantum wires) through which a particle (usually an electron) can move subject to the laws of quantum mechanics (the assumption of independent particles is adopted throughout). Part of the wires are free, in which case the electron wave function is a linear combination of plane waves with wave number k equal to the Fermi momentum k_F and energy $\varepsilon=k_F^2$. From a quantum-mechanical point of view, these wires are good conductors. The other part of the wires are not free in the sense that on each bond there is an attractive or repulsive potential v_j (here j is the bond index; the potential v_j is constant in space along each bond, but may be different from bond to bond) such that the local wave number in these wires is not k but $k_j=(k^2-v_j)^{1/2}$. When $v_j>k^2$ the wave number in bond j is purely imaginary and the motion of the electron is governed by quantum-mechanical tunneling. From a quantum-mechanical point of view, these wires are poor conductors (or insulators). In fact, we will focus our attention on the special situation where v_i is so large that an insulating bond does not carry any current. It can be shown that this particular case corresponds to a model of occupied and missing links. It can be realized simply by removing part of the bonds with some probability, whereas the remaining (occupied) bonds are considered as clean waveguides. This model will be referred to as a percolating lattice of quantum wires. The underlying geometrical framework of the present research is therefore percolation theory, and we will hence make use of the associated concepts of critical behavior, scaling, and fractality. Physically, such quantum-mechanical systems belong to the category of (binary) disordered materials (instead of binary disorder, we can introduce other types of disorder by considering the potential v_j as a random number on each link). Therefore, the underlying physical framework of the present research is localization theory

and the Anderson metal-insulator transition. The main goal of the present study is to combine the concept of electrical-percolation theory (familiar essentially as a classical phenomenon) with the concept of the Anderson transition. To be more specific, imagine that the conductors are distributed randomly on all the bonds of the lattice with probability p (hence the insulators or missing links are distributed randomly with the complementary probability $q=1-p$). Then there is a percolation threshold for $d>1$, namely, a critical value p_c of the occupation probability of the bonds. For $p<p_c$ the conductors only form finite clusters. When p is larger than p_c, there is an infinite cluster of conductors (which is known to be unique in the usual thermodynamical sense). At $p=p_c$ exactly, the infinite cluster (called the incipient infinite cluster) is a fractal object. The quantum-mechanical electrical conductance of such a system is the main object of the present study.

In the present research we are inspired and motivated by the substantial progress in the field of classical theory of electrical percolation (see references below). The essential difference between the classical and quantum-mechanical conductances is related to the concept of localization. We therefore expect an Anderson metal-insulator transition of the quantum-mechanical conductance for $d>2$ only, while such a transition occurs in the classical case also for $d=2$. Moreover, the threshold for quantum-mechanical conductance (denoted hereafter by p_q) will be in general higher than the threshold for classical conductance, which coincides with the geometrical threshold p_c introduced above. Indeed, because of quantum-mechanical localization, the electron wave function may fall off exponentially on the infinite cluster and there will be no transmission even if the system is not cut into pieces. To summarize, the quantum-mechanical threshold probability p_q is nontrivial only in $d>2$ dimensions, while p_c is nontrivial for $d>1$. This difference between the classical and quantum-mechanical problems is schematically depicted in Fig. 1. A second difference is that, in the classical case, what counts is the backbone of the infinite cluster (obtained by removing all the dead ends), whereas in the quantum-mechanical case the whole cluster is relevant since waves are reflected from the dead ends. It should also be emphasized that in the quantum-mechanical problem the electron's energy is an additional parameter and the transmission (conductance) occurs only within an energy band.

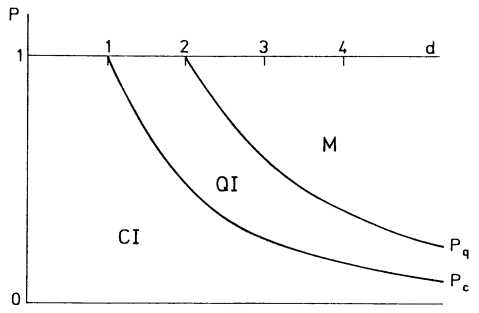

FIG. 1. Schematic phase diagram showing p_c and p_q for a fixed energy, as a function of dimension. CI, classical insulator; QI, quantum insulator; and M, metal.

Geometrical-percolation theory and its applications have already been the subject of a vast number of topical publications and review articles. A monograph by Stauffer[1] provides a complete review of the geometrical aspects of the percolation problem. We cite here briefly a few results relevant for the present research. Consider the percolation probability $P(p)$ defined as the probability that a given bond of the lattice belongs to the infinite cluster. As the variable $\Delta\equiv p-p_c$ approaches 0^+, the quantity $P(p)$ vanishes as Δ^β, where β is the pertinent critical exponent. A second critical exponent ν is related to the two-point correlation function $G(x)$, defined as the probability that two points of the lattice whose relative distance is x are connected by at least one path of occupied bonds. Then $G(x)$ falls off exponentially with $|x|$, and the corresponding correlation length $\xi(p)$ diverges at percolation threshold as $|\Delta|^{-\nu}$. It can be shown by means of general arguments of universality that there are only two independent critical exponents in the geometrical-percolation problem, namely, β and ν. For a d-dimensional system, the fractal dimension of the incipient infinite cluster at $p=p_c$ is $d_f=d-\beta/\nu$.

On the other hand, less is known about electrical percolation. Even in the classical case of a binary lattice of resistors, there are only a few rigorous results concerning the electrical properties of percolating systems. These works and others are summarized in a recent review article by Clerc *et al.*, in which many references can be found.[2] Here again we briefly cite a few results relevant for the present research. If only the occupied bonds have a finite conductance σ, then for $p\rightarrow p_c^+$ the conductivity Σ of the infinite system behaves as Δ^t, where t is the critical exponent of the conductor-insulator mixture. On the other hand, if the links of the missing bonds are now endowed with a finite conductance σ, while the occupied bonds become superconductors, we have a random superconductor-conductor mixture. In this case Σ diverges as $|\Delta|^{-s}$ when p approaches p_c from below. The critical exponents s and t are novel universal characteristics of the percolation problem. They are not related in any simple way to the geometrical exponents β and ν. Several approximate heuristic relations between s, t, β, and ν have been proposed, one of the most celebrated being the Alexander-Orbach[3] conjecture.

Quantum-mechanical percolation effects in disordered electronic systems have been studied by a number of authors: de Gennes, Lafore, and Millot,[4] Kirkpatrick and Eggarter,[5] Odagaki,[6] Raghavan,[7] Shapir, Aharony, and Harris,[8] Meir, Aharony, and Harris,[9] Deutscher, Lévy, and Souillard,[10] Lévy and Souillard,[11] Root and Skinner,[12] Pimentel and de Queiroz,[13] Lambert and Hughes,[14] and others. Most of these works are based on the tight-binding Anderson model of electron localization. To the best of our knowledge, percolation of quantum-mechanical conductance on a binary network of wires has not yet been studied. Beside its significance as an as-yet unknown aspect of percolation theory and fractal structures, the following work may be related to some practical situations, namely, propagation of sound waves

in a system of pipes or propagation of light in a network of optical fibers.

So far, we have been unable to obtain analytical results pertaining to the infinite random system. This is not surprising, since analytical solutions for quantum-mechanical problems in disordered systems are very unlikely to exist for $d > 1$. Therefore, we have to resort to numerical calculations within finite systems of moderate size. On the other hand, the scaling laws discussed above are valid only in the thermodynamic limit. Thus, in order to answer the questions posed above, we have to rely on finite-size-scaling arguments which relate quantities pertaining to a finite system to those of the infinite one using renormalization-group concepts. The finite-size-scaling hypothesis for the conductivity of the classical problem can be stated as follows: For a cubic lattice with lattice constant a and side La (where L is an integer) in d dimensions, the mean classical conductivity $\Sigma_L(p)$ is expected to have the following behavior in the critical region ($|\Delta| = |p - p_c|$ small and L large):

$$\Sigma_L(p) \approx L^{-t/\nu} F(\Delta L^{1/\nu}) , \tag{1.1}$$

where F is a scaling function. The theory of finite-size scaling, developed first on a heuristic basis,[15] has been applied to a very wide verity of physical problems in various geometries.[16,17] The finite-size-scaling hypothesis (1.1) will play the central role in Sec. V, where we will analyze the results of our simulations of the quantum-mechanical conductance for which the threshold probability p_q and critical exponent ν will be evaluated.

Some interesting questions arise in this context which we discuss and answer: Is there a critical behavior of the dc conductance near the percolation threshold? If so, how are the critical exponents related to the classical ones? Does the conductance near threshold obey a scaling law? What is the dependence of the quantum-mechanical threshold probability p_q on energy? Is there a percolation transition in two dimensions as some authors argue? Is there a scaling law controlling the crossover between the diffusive and insulating regimes?

Our principal result is that the conductance follows a finite-size-scaling hypothesis (1.1) compatible with the approximate equality of the critical exponents t and ν. This equality of the critical exponents (a special feature of the quantum-mechanical problem) is not shared by the classical conductivity, but is consistent with the results of nonlinear σ models of localization theory.[18] Furthermore, our results are consistent with the absence of transition in $d = 2$, stressing the fact that the quantum-percolation transition is nothing but an Anderson transition. When the bond-occupation probability approaches 1, we describe the crossover between the disordered (diffusive or metallic) regime and the ordered (ballistic) phase and suggest a scaling law in this regime (p close to 1). We also derive some analytical results pertaining to the ordered system and to a Bethe lattice of quantum wires. Other interesting questions which we do not study but discuss briefly at the end concern the quantum-mechanical ac conductance, the dependence of the ac critical behavior on the frequency, and the influence of magnetic field on all the pertinent quantities.

This paper is organized as follows: In Sec. II we introduce the underlying model, a lattice of quantum wires, which will be the basis for analytical and numerical simulations of two- and three-dimensional ordered and disordered percolating systems. In Sec. III we digress and describe the analytic solutions pertaining to the ordered lattices. As it turns out, the ordered case is interesting and illustrative by itself. It has a nontrivial Bloch dispersion relation, and the conductance of quasi-one-dimensional systems is quantized. An analytic expression for the transmission through a Bethe lattice (Cayley tree) of quantum wires is also presented in this section. The reader who is mainly interested in the disordered case can skip Sec. III without losing contact.

When the system is disordered or percolating, analytic solutions do not exist and a numerical algorithm for the evaluation of the conductance must be constructed. This is carried out in Sec. IV. Special attention is paid to the insulating regime, where the conductance is very small and the use of a transfer matrix is not safe. Then in Sec. V we analyze the numerical results and evaluate the quantum-percolation threshold as well as the critical behavior of the conductance. A brief summary is given in Sec. VI and some open questions are discussed therein.

II. LATTICE OF QUANTUM WIRES

The present model can be considered as a system of narrow waveguides which intersect each other. We take the limit in which the transverse size of each waveguide tends to zero, so that the motion between intersections is virtually one dimensional. In this limit there is no underlying simple Hamiltonian. The basic symmetry and conservation laws of quantum mechanics determine the motion completely once the matching conditions at each intersection are specified. Similar concepts have been used by Avron *et al.*[19] in their study of adiabatic networks. For simplicity of presentation, the number of space dimensions is fixed at $d = 2$ for the illustrative part (figures, etc.). Our numerical calculations are carried out for $d = 2$ and 3.

Consider then a square lattice of one-dimensional wires with lattice spacing a, through which an electron can move subject to the laws of quantum mechanics. In the most general case, there is a wave number k_j on each bond j of the lattice. From this general case it is possible to study several particular situations: (1) If all k_j are real and random, we have a disordered system for which the disorder induces phase randomization. (2) If some of the k_j are purely imaginary, there is a combination of disorder and tunneling. (3) If part of the wires has a wave number k_1 (with probability p) and the other part of the wires has a wave number k_2 (with probability $q = 1 - p$), we have a binary disordered system. (4) If one part of the bonds there are wires with wave number $k = k_F$ (with probability p) and the other part of the bonds is missing, we have a diluted or percolating lattice of quantum wires. We will consider first the model in its general form [cases (1) or (2) above]. The special system of percolating lattice [case (4) above] will be studied in Sec. IV.

In Fig. 2 we depict a finite lattice of length La and width Na. A site can therefore be labeled by a pair of numbers (l,n). An electron can travel on each bond (wire) subject to the laws of quantum mechanics. We will employ the index j for a general bond (horizontal or perpendicular) and n for horizontal bonds only. Thus, if the wave number on a certain bond j ($j=1,2,\ldots,LN$) is k_j, the electron's wave function on this bond is a linear combination of plane waves,

$$\psi_j = a_j e^{ik_j x} + b_j e^{-ik_j x} , \tag{2.1}$$

where, for horizontal (vertical) bonds, the coordinate x is measured from the left (down) site. Imagine now that the N sites on the left of the lattice [these are the sites $(1,n)$] and the N sites on the right of the lattice [these are the sites (L,n)] are connected to electron reservoirs by free wires; namely, the electron's wave number on these wires is $k=k_F$, which is the Fermi wave number. Then we have a quantum-mechanical system whose conductance G (at zero temperature) can be defined in the following way. Let an incoming wave e^{ikx} of unit amplitude reach a site $(1,n)$ on the left column of the lattice. Then the wave function at the mth exit wire on the right [namely, to the right of site (L,m)] will be $t_{mn}e^{ikx}$, where t_{mn} are the elements of the complex transmission matrix $\underline{t}$. Likewise, the wave function at the mth exit wire on the left [namely, to the left of site $(1,m)$] will be $r_{mn}\,e^{-ikx}$, where r_{mn} are the elements of the complex reflection matrix $\underline{r}$. Unitarity (current conservation) implies the equality

$$\underline{t}\,\underline{t}^{\dagger}+\underline{r}\,\underline{r}^{\dagger}=\underline{t}^{\dagger}\underline{t}+\underline{r}^{\dagger}\underline{r}=\underline{I}_N , \tag{2.2}$$

where $\underline{I}_N$ is the $N\times N$ unit matrix.

The linear-response theory now relates the dc conductance G to the transmission in a simple way.[20] One version which we adopt here is

$$G=\frac{e^2}{h}\mathrm{Tr}(\underline{t}\,\underline{t}^{\dagger})\equiv\frac{e^2}{h}g , \tag{2.3}$$

where g is the dimensionless conductance, which, in this formulation, is identical with the transmission coefficient.

Thus, unlike the classical situation in which conductances combine rationally to one another (either in parallel or in series), the situation here is much more complicated, since at each intersection the wave function must be matched according to the rules of continuity and current conservation. Let ψ_1, ψ_2, ψ_3, and ψ_4 be the wave functions of the electron in the four links connected by a given site. The four respective wave numbers are denoted by k_1, k_2, k_3, and k_4, respectively. Then, at this site, the following continuity equation should be satisfied:

$$\psi_1=\psi_2=\psi_3=\psi_4 . \tag{2.4}$$

The relation between derivatives at the intersection is somewhat arbitrary as long as it is compatible with current conservation. For simplicity and consistence with previous work,[19] we will assume the relation

$$\psi_1'+\psi_2'=\psi_3'+\psi_4' , \tag{2.5}$$

where, following Eq. (2.1),

$$\psi_j'=k_j(a_j e^{ik_j x}-b_j e^{-ik_j x}) . \tag{2.6}$$

The relations give four equations relating the coefficients a_j,b_j of Eq. (2.1) of the plane waves on each of the four links.

The most natural algorithm by which one can evaluate the conductance is the transfer-matrix method. After a straightforward algebraic procedure, it is possible to relate the $2N$ coefficients a_n,b_n ($n=1,2,\ldots,N$) pertaining to the horizontal links at column $l+1$ with the $2N$ coefficients a_n,b_n ($n=1,2,\ldots,N$) pertaining to the horizontal links at column l ($l=1,2,\ldots,L-1$). The coefficients a_n,b_n pertaining to the vertical links ($n=1,2,\ldots,N$ or $N-1$ according to the choice of periodic- or free-boundary conditions) have thereby been eliminated. This relation can formally be written as

$$\underline{T}_l\begin{bmatrix}\mathbf{a}\\ \mathbf{b}\end{bmatrix}_l=\begin{bmatrix}\mathbf{a}\\ \mathbf{b}\end{bmatrix}_{l+1} , \tag{2.7}$$

where the $2N\times 2N$ matrix $\underline{T}_l$ is the local transfer matrix, while $\mathbf{a}$ stands for an N-dimensional vector $(a_1,a_2,\ldots,a_N)$, and similarly $\mathbf{b}$ stands for an N-dimensional vector $(b_1,b_2,\ldots,b_N)$. The total transfer matrix $\underline{T}$ relating the $2N$ coefficients $a_n b_n$ ($n=1,2,\ldots,N$) pertaining to the horizontal links at the first column to those at the last column is the product of all the local transfer matrices, namely,

$$\underline{T}=\underline{T}_L\underline{T}_{L-1}\cdots\underline{T}_2\underline{T}_1 . \tag{2.8}$$

The transfer-matrix formalism is sometimes more convenient than a direct evaluation of the transmission matrix. From the knowledge of the transfer matrix, it is then possible to evaluate the dimensionless conductance g using a formula introduced by Pichard,[21] which is equivalent to the expression of the conductance in terms of the transmission matrix [Eq. (2.3)],

$$g=2\,\mathrm{Tr}[(\underline{T}^{\dagger}\underline{T}+\underline{J}_{2N}\underline{T}^{\dagger}\underline{T}\,\underline{J}_{2N}+2\underline{I}_{2N})^{-1}] , \tag{2.9}$$

in which $\underline{I}_{2N}$ is the $2N\times 2N$ unit matrix and $\underline{J}_{2N}$ is a $2N\times 2N$ diagonal matrix with $[\underline{J}_{2N}]_{nn}=1$ for $n=1,2,\ldots,N$, while $[\underline{J}_{2N}]_{nn}=-1$ for $n=N+1,N+2,\ldots,2N$.

Sometimes, however, the transfer-matrix formalism is

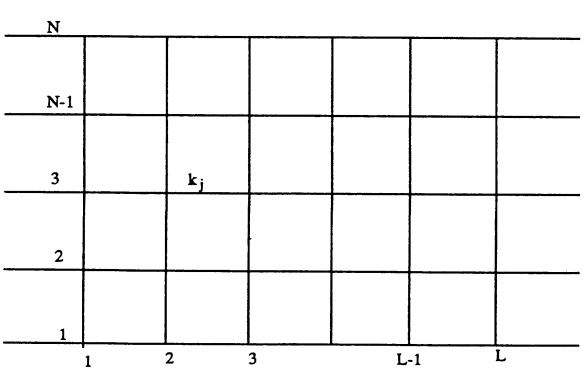

FIG. 2. Two-dimensional lattice of quantum wires.

numerically unstable, and we prefer to make use of a combination of transmission-matrix evaluation and multiple-scattering algorithm developed within the theory of waveguides and filters.[22] Recently, it has been adapted for studying conductances in the insulating regime.[23] This algorithm is explained in Sec. IV.

III. ANALYTIC SOLUTIONS FOR THE PERFECT CRYSTAL

In this section we digress from the main line of the present study and consider the ordered phase of the model for which all links are present. In Sec. III A we will assume that the system stretches to infinity in all dimensions and evaluate the dispersion relation $\varepsilon(\mathbf{q})$, expressing the energy bands in terms of the lattice momenta within the framework of the Bloch theory. In Sec. III B we will start from a system of finite extent, $N^{d-1}\times L$, compute its conductance, and then take the thermodynamic limit. Finally, in Sec. III C we solve the problem of transmission through a Bethe lattice. Since we want eventually to present analytical results, some of the steps below involve tedious but rather straightforward algebraic manipulations. We have therefore chosen to skip technical steps when they are not necessary.

A. Bloch waves and dispersion relation

Analytic expressions for crystal energies in terms of the crystal momenta are very rare. In one dimension the most familiar result is the one due to Kronig and Penney, corresponding to a sequence of rectangular potential barriers. In more than one dimension, the most widely known result is that based on the tight-binding model for free electrons. For the cubic lattice (of constant a) in d dimensions, the energy is given (in some units) by

$$\varepsilon(\mathbf{q})=\sum_{n=1}^{d}\cos(q_n a)\ . \tag{3.1}$$

This simple form results from the complete independence of the motion in all d directions since there is no coupling between the various modes. On the other hand, this is not the case for the perfect lattice of wires since the matching conditions at each site introduce coupling between the various modes. The authors are unaware of a model where all modes are coupled whose energy function is given in a closed (analytical) form. For the present model such a relation exists, as we are now going to show.

Consider a tetragonal lattice in d space dimensions. We will develop our formalism for an anisotropic lattice with lattice constants u_n ($n=1,2,\ldots,d$). Let us concentrate on a site (illustrated in Fig. 3 for $d=2$). There are d pairs of links meeting at the site such that the two links in each pair lie on the same straight line. To any link we then assign a pair of indices (n,i). The first index corresponds to the pair ($n=1,2,\ldots,d$), and the second index labels the link within the corresponding pair ($i=1,2$). With the notation $k=[\varepsilon(\mathbf{q})]^{1/2}$, the matching equations (2.4)–(2.6) at the pertinent site now read

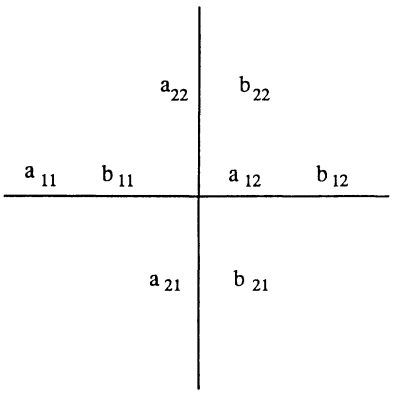

FIG. 3. Intersection of four wires at a site.

$$\begin{aligned} &a_{n1}e^{iku_n}+b_{n1}e^{-iku_n}=a_{n2}+b_{n2}\equiv f\ , \\ &\sum_{n=1}^{d}(a_{n1}e^{iku_n}-b_{n1}e^{-iku_n}+a_{n2}-b_{n2})=0\ , \end{aligned} \tag{3.2}$$

where f is independent of n. The Bloch condition on the wave function is equivalent to the relations

$$a_{n2}=a_{n1}e^{iq_n u_n},\quad b_{n2}=b_{n1}e^{iq_n u_n}\ . \tag{3.3}$$

Equation (3.3) and the first of Eqs. (3.2) now yield

$$\begin{aligned} \frac{a_{n1}}{e^{i(k-q_n)u_n}-1}&=-\frac{b_{n1}}{e^{-i(k+q_n)u_n}-1} \\ &=-\frac{f}{2ie^{-iq_n u_n}\sin(ku_n)}\ . \end{aligned} \tag{3.4}$$

We express all the coefficients in terms of the constant f and substitute into the second of Eqs. (3.2), with the result

$$\sum_{n=1}^{d}\frac{\cos(q_n u_n)-\cos(ku_n)}{\sin(ku_n)}=0\ . \tag{3.5}$$

Equation (3.5) is the desired dispersion relation for the anisotropic lattice. If the lattice is isotropic ($u_n=a=1$), the result simplifies to

$$\cos(k)=\frac{1}{d}\sum_{n=1}^{d}\cos(q_n)\ , \tag{3.6}$$

from which $\varepsilon(\mathbf{q})$ can be expressed in an explicit form. As a result of the coupling introduced in this model, the energy is no longer given by a simple sum as in Eq. (3.1). The energy bands touch each other at the corners of the Brillouin zone, so that there is no energy gap in this model. The density of states is maximal at the middle of each band ($k=\pi/2+m\pi$) and vanishes at its end points ($k=m\pi$). Note also that, as $\mathbf{q}\to\mathbf{0}$, the energy

$$\varepsilon(\mathbf{q})=k^2=\mathbf{q}^2/d+O(\mathbf{q}^4) \tag{3.7}$$

approaches the energy of a free particle whose momentum is equal to the lattice momentum in appropriate units.

B. Conductance of a finite system

In this subsection we study the conductance of a perfect lattice of wires of finite size. The calculations below will be demonstrated in two dimensions for a rectangular lattice of length L (times a lattice constant a) and width N (times a lattice constant b). Extension to d dimensions (length L and transverse cross section N^{d-1}) is straightforward. For an ordered system, the transfer-matrix approach is very useful since it requires the evaluation of a power of a constant matrix.

To fix our notations, we number the horizontal wires of the system from 1 to N and the vertical wires from 1 to L. Let us concentrate on a fixed column of sites (a vertical wire). The wave function on a horizontal link n to the left of this wire is determined by the pair of coefficients a_{n1} and b_{n1}, while on the horizontal link n to the right of this wire it is determined by the pair of coefficients a_{n2} and b_{n2}. The $2N\times 2N$ matrix which transforms the column $\binom{a_{n1}}{b_{n1}}$ into the column $\binom{a_{n2}}{b_{n2}}$ is denoted by $\underline{M}$ and will be evaluated below. To implement the propagation of the wave from column i to column $i+1$ ($i=1,2,\ldots,L-1$), one has to multiply the column $\binom{a_{n2}}{b_{n2}}$ by the phase matrix ω to be defined below. The transfer matrix transforming the wave function from vertical wire i to its neighbor wire $i+1$ is just the product $\underline{S}=\underline{\omega}\,\underline{M}$. Thus we write

$$\begin{bmatrix} a_{n2} \\ b_{n2} \end{bmatrix} = \underline{M} \begin{bmatrix} a_{n1} \\ b_{n1} \end{bmatrix}, \quad \underline{S}=\underline{\omega}\,\underline{M} \ , \qquad \underline{\omega} = \begin{bmatrix} e^{ika}\underline{I}_N & \underline{0} \\ \underline{0} & e^{-ika}\underline{I}_N \end{bmatrix} , \tag{3.8}$$

where $\underline{I}_N$ is the unit matrix in the pertinent space. Since the system is ordered, the transfer matrix from one side of the system to the other side is

$$\underline{T}=\underline{S}^L \ . \tag{3.9}$$

Conservation of current (unitarity) imposes the following relation on T:

$$\underline{T}^\dagger \underline{J}_{2N} \underline{T} = \underline{J}_{2N}, \quad \underline{J}_{2N} = \begin{bmatrix} \underline{I}_N & \underline{0} \\ \underline{0} & -\underline{I}_N \end{bmatrix} . \tag{3.10}$$

Similar relations apply also to $\underline{M}$ and $\underline{\omega}$.

From the knowledge of the transfer matrix of the system, one can evaluate the conductance $G=(e^2/h)g$ using Pichard's formula (2.9).[21]

Our first task is to find the matrix $\underline{M}$ appearing in Eq. (3.8). This is achieved by eliminating the coefficients of the plane waves on the vertical links in terms of the corresponding coefficients on the horizontal links using the matching equations on the wave function. After the result of this procedure is inserted in the equation for the current conservation (relating the derivatives of the wave function), the desired linear relation between the coefficients of the wave function on the left side and those on the right side is obtained. The result is then

$$\underline{M} = \begin{bmatrix} \underline{I}_N + i\underline{A} & i\underline{A} \\ -i\underline{A} & \underline{I}_N - i\underline{A} \end{bmatrix} , \tag{3.11}$$

where $\underline{A}$ is a real $N\times N$ symmetric matrix. If we adopt free-boundary conditions in the transverse direction, we find

$$\begin{aligned} A(n,n+1) &= \tfrac{1}{2}\csc(kb) \quad (n=1,2,\ldots,N-1) \ , \\ A(n,n) &= -\cot(kb) \quad (n=1,2,\ldots,N) \ . \end{aligned} \tag{3.12}$$

Note the similarity with the kinetic-energy matrix in the tight-binding model, which has the value -2 on the diagonal and 1 near the diagonal, with all other elements being zero. We will now carry out the following manipulations: (1) diagonalization of the matrix $\underline{A}$ defined in Eq. (3.12); (2) diagonalization of the transfer matrix $\underline{S}=\underline{\omega}\,\underline{M}$, where $\underline{\omega}$ is the diagonal matrix of phases defined in Eq. (3.8) and the matrix $\underline{M}$ is defined in Eq. (3.11); (3) find $\underline{T}=\underline{S}^L$ and $\underline{T}^\dagger=(\underline{S}^\dagger)^L$ and diagonalize the matrix $\underline{T}^\dagger\underline{T}$; (4) use the eigenvalues of $\underline{T}^\dagger\underline{T}$ to compute the conductance.

Starting with step (1), we write the eigenvalue equation $\underline{A}\mathbf{v}=\lambda\underline{I}\mathbf{v}$ as

$$2\sin(kb)\lambda v_n = v_{n+1}+v_{n-1}-2\cos(kb)v_n \qquad (n=1,2,\ldots,N) \ , \tag{3.13}$$

and the free-boundary conditions are implied by the equalities $v_{N+1}/v_N=v_0/v_1=\cos(kb)$. We now look for N solutions for the eigenvectors $\mathbf{v}(q)=[v_1(q),v_2(q),\ldots,v_N(q)]^\dagger$, and the corresponding eigenvalues $\lambda(q)$ (where the index q, which labels the solution, can get N values $q_1,q_2,\ldots,q_N$). These solutions are of the form

$$\begin{aligned} v_n(q) &= \alpha\cos(nqb)+\beta\sin(nqb) \ , \\ \lambda(q) &= \frac{\cos(qb)-\cos(kb)}{\sin(kb)} \ , \end{aligned} \tag{3.14}$$

which leads to the following homogeneous set of equations for the constants α and β:

$$\begin{aligned} \alpha &= \cos(kb)[\alpha\cos(qb)+\beta\sin(qb)] \ , \\ \alpha\cos[(N+1)qb]+\beta\sin[(N+1)qb] &= \cos(kb)[\alpha\cos(Nqb)+\beta\sin(Nqb)] \ . \end{aligned} \tag{3.15}$$

Eliminating the coefficients α and β, we then get a secular equation for the momenta q:

$$\sin[(N+1)qb]-2\cos(kb)\sin(Nqb)+\cos^2(kb)\sin[(N-1)qb]=0 \ . \tag{3.16}$$

Now let us recall that

$$\sin(mqb)=\sin(qb)P_m(x), \quad x=2\cos(qb) \ , \tag{3.17}$$

where the $P_m(x)$ are a polynomials of degree $m-1$ in x [related to Chebyshev polynomials of the second kind U_k through the relation $P_m(x)=U_{m-1}(\frac{1}{2}x)$]. They satisfy the recursion relation

$$P_{m+1}+P_{m-1}=xP_m \ . \tag{3.18}$$

Substitution of Eq. (3.17) in Eq. (3.16) yields the relation

$$P_{N+1}-2\cos(kb)P_N+\cos^2(kb)P_{N-1}=0 \ . \tag{3.19}$$

The left-hand side of Eq. (3.19) is a polynomial of degree N in $x=2\cos(qb)$, whose N roots x_m define the corresponding eigenmomenta q_m $(m=1,2,\ldots,N)$. Since the matrix $\underline{A}$ is symmetric, its eigenvalues must be real and $|x_m|\le 2$. Following Eq. (3.14), we write the eigenvalues of $\underline{A}$ as

$$\lambda_m=\frac{\gamma_m}{\sin(kb)}, \quad \gamma_m=\tfrac{1}{2}x_m-\cos(kb) \ . \tag{3.20}$$

Before passing to the next step, we mention that if one adopts periodic-boundary conditions in the transverse direction, the evaluation of the eigenvalues λ_m is much simpler with the result $q_m=2\pi m/N$.

In order to complete the diagonalization procedure, we must also consider the matrix $\underline{V}$ which diagonalizes $\underline{A}$, such as

$$\begin{aligned}&\underline{A}=\underline{V}^T\underline{\Lambda}\,\underline{V}, \quad \underline{V}^T\underline{V}=\underline{V}\,\underline{V}^T=\underline{I}_N \ , \\ &\underline{\Lambda}=\mathrm{diag}(\lambda_1,\lambda_2,\ldots,\lambda_N) \ .\end{aligned} \tag{3.21}$$

Fortunately, as we show below, the matrix of eigenvectors does not enter into the expression for the conductance [Eq. (2.9)]. Indeed, we may use the $N\times N$ matrix V to define a $2N\times 2N$ matrix U which transforms the matrix $\underline{M}$ [Eq. (3.11)] into the polar representation

$$\begin{aligned}&\underline{M}=\underline{U}^T\underline{\Delta}\,\underline{U}, \quad \underline{U}=\begin{pmatrix}\underline{V} & \underline{0}\\ \underline{0} & \underline{V}\end{pmatrix} \ , \\ &\underline{U}^T\underline{U}=\underline{U}\,\underline{U}^T=\underline{I}_{2N}, \quad \underline{\Delta}=\begin{pmatrix}\underline{I}_N+i\underline{\Lambda} & i\underline{\Lambda}\\ -i\underline{\Lambda} & \underline{I}_N-\underline{\Lambda}\end{pmatrix} \ .\end{aligned} \tag{3.22}$$

The same matrix $\underline{U}$ is also employed when we write the transfer matrix $\underline{S}=\underline{\omega}\,\underline{M}$ [Eq. (3.8)], which is required to transform the coefficients from one column of sites to its neighbor. Thus

$$\underline{S}=\underline{U}^T\underline{\tau}\,\underline{U}, \quad \underline{\tau}=\underline{\omega}\,\underline{\Delta} \ . \tag{3.23}$$

Hence, for the total transfer matrix $\underline{T}$ through L columns of sites [Eq. (3.9)], we have

$$\underline{T}=\underline{U}^T\underline{\tau}^L\underline{U}, \quad \underline{T}^\dagger=\underline{U}^T\underline{\tau}^{\dagger L}\underline{U}, \quad \underline{T}^\dagger\underline{T}=\underline{U}^T\underline{\tau}^{\dagger L}\underline{\tau}^L\underline{U} \ . \tag{3.24}$$

Therefore, the conductance [Eq. (2.9)] is equal to

$$\begin{aligned}g&=2\,\mathrm{tr}[\underline{\tau}^{\dagger L}\underline{\tau}^L+(\underline{\tau}^{\dagger L}\underline{\tau}^L)^{-1}+2\underline{I}_{2N}]^{-1} \\ &=2\sum_{m=1}^{2N}\frac{\mu_m}{(\mu_m+1)^2} \ ,\end{aligned} \tag{3.25}$$

where μ_m are the eigenvalues of the matrix $\underline{\tau}^{\dagger L}\underline{\tau}^L$.

Equation (3.19) and (3.21) then complete the first step, namely, the diagonalization of the matrix $\underline{A}$. Moreover, from the structure of the matrix $\underline{M}$ [Eq. (3.22)], it is clear that the task of the second step (diagonalization of $\underline{S}=\underline{\omega}\,\underline{M}$) is equivalent to the diagonalization of $\underline{\tau}=\underline{\omega}\,\underline{\Delta}$ [Eq. (3.23)]. This procedure as well as steps (3) and (4) can be achieved by a separate algebraic manipulation on any one of the N 2×2 matrices,

$$\begin{aligned}\alpha&=\begin{pmatrix}e^{ika} & 0\\ 0 & e^{-ika}\end{pmatrix}\begin{pmatrix}1+i\lambda & i\lambda\\ -i\lambda & 1-i\lambda\end{pmatrix} \\ &=\begin{pmatrix}e^{ika}(1+i\lambda) & e^{ika}i\lambda\\ -e^{-ika}i\lambda & e^{-ika}(1-i\lambda)\end{pmatrix} \ ,\end{aligned} \tag{3.26}$$

where the dependence of the matrix $\underline{\alpha}$ and the eigenvalue λ on m $(m=1,2,\ldots,N)$ is dropped henceforth. In order to diagonalize the matrix $\underline{\alpha}$, we note that it belongs to the group SU(1,1) of 2×2 matrices with the structure

$$\underline{\alpha}=\begin{pmatrix}p & q\\ q^* & p^*\end{pmatrix}$$

with $\det(\underline{\alpha})=|p|^2-|q|^2=1$. It is then useful to denote its eigenvalues by $e^{\pm i\theta}$, where θ, defined by

$$\cos\theta=\tfrac{1}{2}\mathrm{tr}(\underline{\alpha})=\cos(ka)-\lambda\sin(ka) \ , \tag{3.27}$$

is real if $|\mathrm{tr}(\underline{\alpha})|\le 2$. Recall that θ depends on the index m of the eigenvalue λ_m of the matrix $\underline{A}$. It is then clear that for a large system $(L\to\infty)$ only those values of m for which θ is real will contribute to the transmission, since eventually we will need to consider the matrix $\underline{\alpha}^L$. These are the open (intrinsic) channels of the system. A channel m for which θ is not real has an exponentially small contribution as $L\to\infty$. We now proceed to diagonalize the matrix $\underline{\alpha}$ and write

$$\underline{\alpha}=\underline{P}\begin{pmatrix}e^{i\theta} & 0\\ 0 & e^{-i\theta}\end{pmatrix}\underline{P}^{-1}\equiv\underline{P}\,\underline{\Theta}\,\underline{P}^{-1} \ . \tag{3.28}$$

The matrices P and P^{-1} are computed after somewhat straightforward but tedious linear-algebraic manipulations with the result

$$P=\begin{pmatrix}1-e^{ika+i\theta} & 1-e^{ika-i\theta}\\ -1+e^{-ika+i\theta} & -1+e^{-ika-i\theta}\end{pmatrix} \ , \tag{3.29}$$

$$P^{-1}=\frac{1}{4\sin(ka)\sin\theta}\begin{pmatrix}1-e^{-ika-i\theta} & 1-e^{ika-i\theta}\\ -1+e^{-ika+i\theta} & -1+e^{ika+i\theta}\end{pmatrix} \ .$$

Following the discussion preceding Eq. (3.27), we have to evaluate the eigenvalues of the matrix $\underline{\alpha}^{\dagger L}\underline{\alpha}^L=(\underline{P}^\dagger)^{-1}(\Theta^\dagger)^L\underline{P}^\dagger\underline{P}\,\underline{\Theta}^L\underline{P}^{-1}$. Actually, we can find these eigenvalues μ from the similar matrix

$$\underline{W}\equiv(\underline{\Theta}^\dagger)^L\underline{P}^\dagger\underline{P}\,\underline{\Theta}^L(\underline{P}_\dagger\underline{P})^{-1} \ . \tag{3.30}$$

The explicit expression for $\underline{W}$ is

$$W=\frac{1}{\sin(ka)[(1-\lambda^2)\sin(ka)+2\lambda\cos(ka)]}\begin{bmatrix} e^{-iL\theta} & 0 \\ 0 & e^{iL\theta}\end{bmatrix}\begin{bmatrix}\sin(ka)+\lambda\cos(ka) & -\lambda e^{-i\theta} \\ -\lambda e^{i\theta} & \sin(ka)+\lambda\cos(ka)\end{bmatrix}$$
$$\times\begin{bmatrix} e^{iL\theta} & 0 \\ 0 & e^{-L\theta}\end{bmatrix}\begin{bmatrix}\sin(ka)+\lambda\cos(ka) & \lambda e^{-i\theta} \\ \lambda e^{i\theta} & \sin(ka)+\lambda\cos(ka)\end{bmatrix}. \tag{3.31}$$

Restoring back the dependence on m through λ_m, it is verified that $\det(\underline{W}_m)=1$ and therefore the contribution of a specific channel m to the conductance g according to Eq. (3.25) equals $4/[2+\mathrm{tr}(\underline{W}_m)]$. Thus, after $\mathrm{tr}(\underline{W}_m)$ is evaluated from Eq. (3.31), we obtain

$$g=\sum_{m=1}^{N}\frac{4}{2+\mathrm{tr}(\underline{W}_m)}$$
$$=\sum_{m=1}^{N}\frac{[\sin(ka)+\lambda_m\cos(ka)]^2-\lambda_m^2}{[\sin(ka)+\lambda_m\cos(ka)]^2-\lambda_m^2\cos^2(L\theta_m)}$$
$$=\sum_{m=1}^{N}\left[1+\frac{\lambda_m^2\sin^2(L\theta_m)}{\sin(ka)[(1-\lambda_m^2)\sin(ka)+2\lambda_m\cos(ka)]}\right]^{-1}. \tag{3.32}$$

The sum is taken on all channels, but as we have indicated, only the open channels defined after Eq. (3.27) contribute significantly for large L. The general result expressed in Eq. (3.32) takes a simpler form in the isotropic case (a square lattice of constant $a=b=1$, say). Then we get from Eqs. (3.20) and (3.27) the relations

$$\lambda_m=\frac{\gamma_m}{\sin k},\quad \gamma_m=\tfrac{1}{2}x_m-\cos k\ ,$$
$$\cos\theta_m=\cos k-\gamma_m=2\cos k-\tfrac{1}{2}x_m\ . \tag{3.33}$$

Restoring the length and width dependence, the conductance g_{NL} becomes

$$g_{NL}=\sum_{m=1}^{N}\left[1+\left[\frac{\gamma_m\sin(L\theta_m)}{\sin\theta_m\sin k}\right]^2\right]^{-1}, \tag{3.34}$$

which is our final result as far as the finite system is concerned.

It is interesting to approach the thermodynamic limit starting from Eq. (3.34). This procedure is meaningful if the order of the two limits on L and N is first $L\to\infty$ and then $N\to\infty$. In the $L\to\infty$ limit, in the isotropic case, the sum on the open channels is restricted to those values of m such that the inequality $\cos\theta_m=2\cos k-\cos q_m\le 1$ holds. It is then useful to define a number $\nu_N(k)$ of open channels for an infinitely long system of width N at a given energy k^2. We will see below that $\nu_N(k)$ gets its maximum near $k=\pi/2$. Note also that if k is replaced by $\pi-k$, then γ_m changes sign [see Eq. (3.33)], but $\nu_N(k)=\nu_N(\pi-k)$. As $L\to\infty$ in Eq. (3.34), we replace $\sin^2(L\theta_m)$ by $\frac{1}{2}$. For the term $\sin^2\theta_m$ in the denominator, we use Eq. (3.33) and recall that $x_m=2\cos q_m$. Thus

$$g_N\equiv g_{NL}(L\to\infty)$$
$$=\sum_m\left[1+\frac{(\cos q_m-\cos k)^2}{2\sin^2 k[1-(2\cos k-\cos q_m)^2]}\right]^{-1}. \tag{3.35}$$

The conductance of an infinitely long sample at a fixed finite width N is plotted in Figs. 4(a) and 4(b) as a function of k between 0 and $\pi/2$. The conductance is quantized in the sense that it jumps by roughly one unit each time a new channel is opened (although the steps are not sharp). This result shows that quantization of conductance occurs not only in the ballistic propagation through narrow constrictions, but also when the electron motion is effected in periodic samples. We also remark that the conductance band starts at $k=0$ and is centered at $k=\pi/2$, in accordance with the result obtained in Sec. III A concerning the energy bands in the framework of Bloch theory.

Before taking the limit $N\to\infty$, it is necessary to estimate the number $\nu_N(k)$ of open channels at energy k^2 in the large-N limit. In this case it can be shown that the solutions q_m of Eq. (3.19) are uniformly spread on the interval $[0,\pi]$ and hence

$$\frac{\nu_N(k)}{N}\approx\frac{1}{\pi}\arccos(2\cos k-1)\equiv\frac{1}{\pi}q_0\ . \tag{3.36}$$

Hence $\nu_N(0)=0$ and $\nu_N(\pi/2)=N$. In between, the function $\nu_N(k)$ increases monotonically. We now effect the large-N limit which (for a single sum over lattice momenta) is done through the usual substitution $N^{-1}\sum_m F(q_m)\to(1/\pi)\int F(q)dq$. Thus

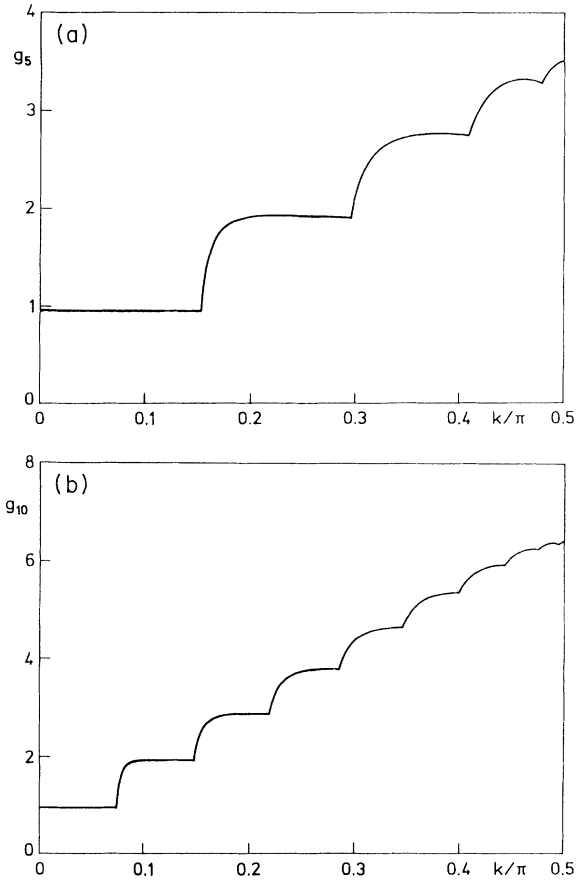

FIG. 4. (a) Conductance g_5 of a two-dimensional ordered lattice of wires of finite length and finite width $N=5$ as a function of the Fermi wave number. (b) Same as (a) with $N=10$.

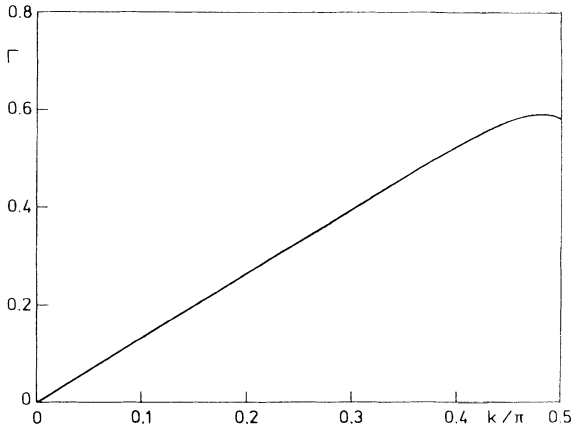

FIG. 5. Conductance Γ per unit transverse width of a two-dimensional ordered lattice of wires of infinite length and large width as a function of the Fermi wave number.

$$\Gamma \equiv \frac{g_N}{N}(N\to\infty) = \frac{g_{NL}}{N}(L\to\infty,\ N\to\infty) \approx \frac{1}{\pi}\int_0^{q_0} dq \left[1+\frac{(\cos q-\cos k)^2}{2\sin^2 k[1-(2\cos k-\cos q)^2]}\right]^{-1} . \tag{3.37}$$

This quantity is plotted as a function of k in Fig. 5. Note that this $\Gamma(k)$ is not strictly monotonic. Yet a rough estimate of the form $g\approx\nu_N(k)$ for finite N and infinite length L is quite reasonable. We also remark that the quantization steps are smoothed out and the conductance per unit width is a smooth function of energy. Its value at the band center ($k=\pi/2$) is easily found to be

$$\Gamma(k=\pi/2)=\frac{1}{\pi}\int_0^{\pi} dq \frac{1-\cos q}{3-\cos q} = 2-\sqrt{2}\approx 0.585\,78 . \tag{3.38}$$

We stress that all the results obtained in this subsection pertain to two-dimensional systems. Extension to $d>2$ is straightforward once the eigenvalues λ_m are given. Thus the sum on all channels in Eqs. (3.32) and (3.34) will include $(d-1)$ transverse indices, while the sum in Eq. (3.35) will extend on all open channels out of the total N^{d-1}. Integrals such as the one appearing in Eq. (3.37) will be $d-1$ dimensional. Thus, for $d=3$, we assume NM transverse channels and get

$$\frac{\nu_{NM}(k)}{NM}\approx\frac{1}{(2\pi)^2}\int dq_y\int dq_z\,\Theta(1-|3\cos k-\cos q_y-\cos q_z|) , \tag{3.39}$$

where $\Theta(x)$ is the Heaviside unit-step function. Finally, the conductance (per unit transverse cross section) of a three-dimensional isotropic lattice in the thermodynamic limit reads

$$\Gamma=\frac{g_{NML}}{NM}(L\to\infty,\ N,M\to\infty)\approx\frac{1}{(2\pi)^2}\int dq_y\int dq_z\,\Theta(1-|3\cos k-\cos q_y-\cos q_z|) \times\left[1+\frac{(2\cos k-\cos q_y-\cos q_z)^2}{2\sin^2 k[1-(3\cos k-\cos q_y-\cos q_z)^2]}\right]^{-1} . \tag{3.40}$$

C. Transmission through a Bethe lattice

It has been established that when the system is ordered, the transmission coefficient of a quasi-one-dimensional structure has a band structure; namely, it equals zero for some energy intervals, and it is greater than zero for other intervals. These intervals are identical to the bands in the pertinent geometry. It has also been demonstrated that when the system is disordered the transmission coefficient for $d \leq 2$ is zero in the thermodynamic limit. The question of what happens "in between," when the system is not ordered but not completely random either, is not yet answered. As an example, we note that for a two-dimensional Penrose tiling, it is believed that the situation is similar (but not identical) to the disordered case in the sense that the transmission is zero for "almost all energies."[24] From this point of view, it is then of some interest to study the transmission through a fractal object. Within the model of quantum wires, the Bethe lattice (equivalently the Cayley tree) is especially easy to investigate. It is found that the transmission coefficient has a band structure which shrinks to zero as the coordination number increases.

We consider (Fig. 6) the problem of quantum wires in the geometry of a symmetric tree with L generations and N branches ($N=z-1$, where z is the coordination number). The generations are counted from each side of the tree toward its axis of symmetry. The number of branches in the lth generation is N^l. If an incoming wave e^{ikx} reaches the system from the leftmost branch, it will be partly reflected back with a reflection amplitude ρ and partly transmitted into the rightmost branch with transmission amplitude τ. Our aim is to compute the transmission coefficient $|\tau|^2$, which is determined through the Pichard formula by the 2×2 matrix $\underline{S}$ transforming the vector $(1,\rho)$ to $(\tau,0)$:

$$|\tau|^2=\frac{4}{2+\mathrm{tr}(\underline{S}^{\dagger}\underline{S})} . \tag{3.41}$$

The matrix $\underline{S}$ can be evaluated by the transfer-matrix algorithm, which involves a successive application of matrices $\underline{T}$ ($\underline{T}^{-1}$) transforming the wave function from generation l on the left (right) of the symmetry axis to generation $l+1$ ($l-1$). On a branch of generation l to the left (right) of the symmetry line, the wave function is written as $a_l e^{ikx}+b_l e^{-ikx}$ ($c_l e^{ikx}+d_l e^{-ikx}$). Because of symmetry, the coefficients of the wave e^{ikx} on all branches belonging the same generation are equal (and similarly for the wave e^{-ikx}). Note that if $(a_0,b_0)=(1,\rho)$, then $(c_0,d_0)=(\tau,0)$. The matrix $\underline{T}$ is calculated using continuity- and current-conservation requirements at the vertex l separating generations l and $l+1$ ($l=0,1,\ldots,L-1$):

$$\begin{aligned} a_l e^{ik}+b_l e^{-ik}&=a_{l+1}+b_{l+1} , \\ a_l e^{ik}-b_l e^{-ik}&=N(a_{l+1}-b_{l+1}) . \end{aligned} \tag{3.42}$$

From these equations the matrix $\underline{T}$ is easily determined:

$$\begin{aligned} &\begin{bmatrix} a_{l+1} \\ b_{l+1} \end{bmatrix}=\underline{T}\begin{bmatrix} a_l \\ b_l \end{bmatrix} , \\ &\underline{T}=\frac{1}{2N}\begin{bmatrix} (N+1)e^{ik} & (N-1)e^{-ik} \\ (N-1)e^{ik} & (N+1)e^{-ik} \end{bmatrix} . \end{aligned} \tag{3.43}$$

Anticipating the need to compute $\underline{T}^L$, we carry out the diagonalization of $\underline{T}$. The eigenvalues of $\underline{T}$ are

$$\lambda_{\pm}=\frac{1}{\sqrt{N}}e^{\pm i\theta}, \quad \cos\theta=\frac{N+1}{2\sqrt{N}}\cos k . \tag{3.44}$$

The range of values of k for which θ is real determine the energy band, namely,

$$\frac{N+1}{2\sqrt{N}}\cos k \leq 1 , \tag{3.45}$$

which is symmetric and centered at $k=\pi/2$. It is then sufficient to consider the interval $0\leq k\leq\pi$. As the order N increases, the energy band becomes narrower and shrinks to zero. We then write

$$\underline{T}=\underline{P}\,\underline{\Delta}\,\underline{P}^{-1} \quad \text{with } \underline{\Delta}=\frac{1}{\sqrt{N}}\begin{bmatrix} e^{i\theta} & 0 \\ 0 & e^{-i\theta} \end{bmatrix} , \tag{3.46}$$

and find for the matrix $\underline{P}$ and its inverse $\underline{P}^{-1}$ the expressions

$$\begin{aligned} \underline{P}&=\begin{bmatrix} (N-1)\cos\theta e^{-ik} & (N-1)\cos\theta e^{-ik} \\ i(N+1)\sin(\theta-k) & -i(N+1)\sin(\theta+k) \end{bmatrix} , \\ \underline{P}^{-1}&=\frac{e^{ik}}{i(N^2-1)\cos k\,\sin(2\theta)} \\ &\quad\times\begin{bmatrix} i(N+1)\sin(\theta+k) & (N-1)\cos\theta e^{-ik} \\ i(N+1)\sin(\theta-k) & -(N-1)\cos\theta e^{-ik} \end{bmatrix} . \end{aligned} \tag{3.47}$$

The propagation of the wave function from the leftmost branch of the tree to the Lth generation situated on the left of the symmetry axis is therefore achieved through the transformation

$$\begin{bmatrix} a_L \\ b_L \end{bmatrix}=\underline{T}^L\begin{bmatrix} a_0 \\ b_0 \end{bmatrix} . \tag{3.48}$$

To cross the symmetry axis, an additional phase should be added, namely,

$$c_L=a_L e^{ik}, \quad d_L=b_L e^{-ik} . \tag{3.49}$$

On the other hand, we may reach the wave function at

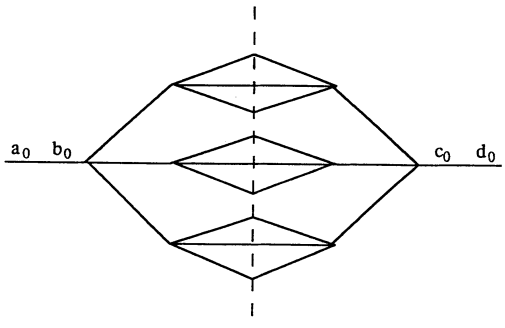

FIG. 6. Bethe lattice with its mirror image for $z=4$, $N=3$, and $L=2$.

points of the generation L situated to the right of the symmetry axis starting from the rightmost branch and propagating backward (from right to left). This backward propagation is again carried out in terms of the matrix $\underline{T}^L$, but the role of leftward and rightward waves is interchanged. Taking account of the relevant phases, the desired backward transformation reads

$$\begin{bmatrix} e^{-ik}d_L \\ e^{ik}c_L \end{bmatrix} = \underline{T}^L \begin{bmatrix} e^{ik}d_0 \\ e^{ik}c_0 \end{bmatrix} . \tag{3.50}$$

Thus we can write the transformation from the leftmost branch to the rightmost branch as

$$\begin{bmatrix} c_0 \\ d_0 \end{bmatrix} = \underline{S} \begin{bmatrix} a_0 \\ b_0 \end{bmatrix} , \tag{3.51}$$

where the matrix S is explicitly given by

$$\underline{S} = \begin{bmatrix} 0 & e^{-ik} \\ e^{ik} & 0 \end{bmatrix} \underline{T}^{-L} \begin{bmatrix} 0 & e^{-2ik} \\ e^{2ik} & 0 \end{bmatrix} \underline{T}^L . \tag{3.52}$$

Using Eqs. (3.46) and (3.47), the successive powers of $\underline{T}$ can easily be evaluated and the product of matrices on the right-hand side of Eq. (3.52) is then carried out. The result is

$$\underline{S} = \frac{1}{4N\sin^2(2\theta)} \begin{bmatrix} F & G \\ G^* & F^* \end{bmatrix} ,$$

$$F = 4(N+1)^2 e^{ik}[\cos k \sin\theta \cos(L\theta) + i \sin k \cos\theta \sin(L\theta)]^2 - 4(N-1)^2 e^{-ik}\cos^2\theta \sin^2(L\theta) , \tag{3.53}$$

$$G = 16i\sqrt{N}(N-1)\sin k e^{-ik}\cos^2\theta \sin(L\theta)\sin[(L+1)\theta] .$$

According to Eq. (3.41), we need the product $\underline{S}^\dagger\underline{S}$, which is

$$\underline{S}^\dagger\underline{S} = \frac{1}{(4N)^2\sin^4(2\theta)} \begin{bmatrix} FF^*+GG^* & 2FG^* \\ 2F^*G & FF^*+GG^* \end{bmatrix} . \tag{3.54}$$

Therefore, we have

$$|\tau|^2 = \frac{4}{2+\mathrm{tr}(\underline{S}^\dagger\underline{S})} = \frac{1}{1+R} ,$$

$$R = \frac{GG^*}{(4N)^2\sin^4(2\theta)} = \frac{(N-1)^2\sin^2 k \sin^2(L\theta)\sin^2[(L+1)\theta]}{N\sin^4\theta} . \tag{3.55}$$

Equation (3.55) is our final result concerning the transmission through a system of finite length L. We will now investigate the limit $L \to \infty$ by replacing the rapidly oscillating function by their average values (denoted by $\langle\ \rangle$). Thus we set

$$\langle \sin^2(L\theta)\rangle = \tfrac{1}{2}, \quad \langle \sin^4(L\theta)\rangle = \tfrac{3}{8} ,$$
$$\langle \sin^2(L\theta)\cos^2(L\theta)\rangle = \tfrac{1}{8} , \tag{3.56}$$

and find

$$\langle \sin^2(L\theta)\sin^2[(L+1)\theta]\rangle = \tfrac{1}{8}(1+2\cos^2\theta) . \tag{3.57}$$

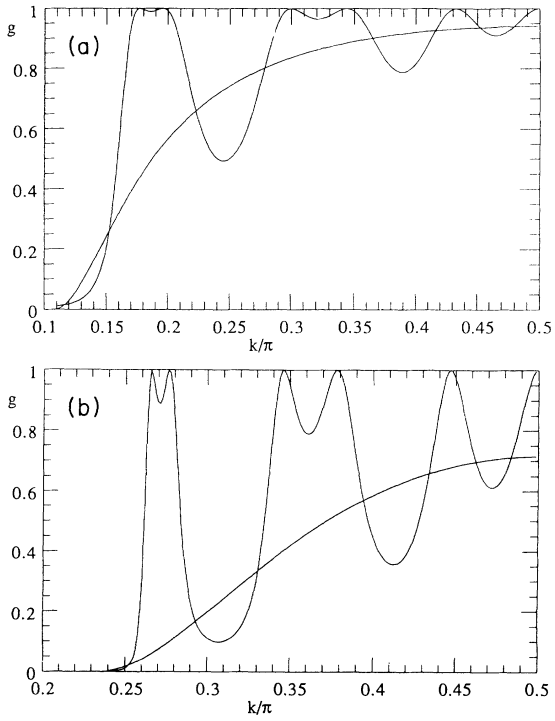

FIG. 7. (a) Conductance of Bethe lattice of coordination number $z=N+1$ and L generations as a function of energy within the band. The oscillatory function corresponds to finite L, while the smooth line corresponds to L infinite. Here $N=2$ and $L=6$. (b) Same as (a) with $N=5$.

Hence we get

$$R_\infty = R(L\to\infty) = \frac{(N-1)^2\sin^2 k(1+2\cos^2\theta)}{8N\sin^4\theta} . \tag{3.58}$$

We note that this result does not make much sense, since the left-hand side of Eq. (3.57) oscillates between 0 and $\frac{1}{4}(1+|\cos\theta|)^2$. Hence, for L large, R oscillates very rapidly between 0 (corresponding to perfect transmission $|\tau|^2=1$) and

$$R_{\max} = \frac{(N-1)^2\sin^2 k(1+|\cos\theta|)^2}{4N\sin^4\theta} , \tag{3.59}$$

for which the transmission is maximally reduced by interference effects. Figure 7 displays the transmission for several values of N,L as a function of k.

We have thus established analytical solutions of the problems pertaining to the ordered system and move on to discuss those related to the disordered system. Inevitably, these solutions will not be analytical, and therefore we need a numerical procedure to solve the scattering problem. This procedure is discussed in the next section.

IV. NUMERICAL SOLUTION

A. General considerations

In this section we will explain how the conductance of the disordered system is evaluated. First, we shall work

it out for the case of random wave numbers on the links, and then we will study the case of missing links (the percolating network). In the first case, the similarity with the tight-binding model may lead us to the desired algorithm for the numerical solution. The most commonly used is the transfer-matrix method. Here, however, we intend to study the system also in the far insulating regime. A transfer-matrix approach is hence dangerous since the product of many matrices will blow up. Furthermore, we intend to study a cubic system with N^3 up to 1000 sites. The size of the (complex) transfer matrix will then be $2N^2=200$, which is quite large. It is then indispensable to invent a method which does not rely on a divergent product of large matrices and at the same time will employ matrices of smaller size. This method is explained below in a heuristic manner. Its rigorous justification goes back to the theory of waveguides.[22] It involves the algebra of transmission and reflection matrices whose size is N^2. The disadvantage here is that each step requires an inversion procedure instead of a simple multiplication as is required by the transfer-matrix algorithm. The advantage of the present procedure is threefold. First, as we have noted, it involves matrices of size N^2 and not $2N^2$. Second, the transmission and reflection matrices are bounded through the unitarity relation, and hence there is no danger of exponential Lyapunov divergence. Third, it can also be applied in the case of missing links in which the concept of a transfer matrix is ill defined.

Consider then a wave approaching a system of two barriers 1 and 2. The transmission and reflection amplitudes for each individual barrier i ($i=1,2$), independent of the other one, are assumed to be given by $\underline{t}_i$ and $\underline{r}_i$ if the wave approaches the barrier from the left and by $\underline{t}'_i$ and $\underline{r}'_i$ if the wave approaches the barrier from the right. For a multichannel problem, the transmission and reflection amplitudes are complex matrices. The situation where the number of incoming channels (N) is different from the number of outgoing channels (M) requires some care. We stick to the notation in which the right (left) index of a matrix corresponds to an incoming (outgoing) channel. The dimensions of $\underline{t}_i$, $\underline{r}_i$, $\underline{t}'_i$, and $\underline{r}'_i$ (for a given barrier i) are then $M\times N$, $N\times N$, $N\times M$, and $M\times M$, respectively. They are usually arranged in an $\underline{S}$ matrix pertaining to barrier i:

$$\underline{S}_i=\begin{bmatrix}\underline{t}_i & \underline{r}'_i\\ \underline{r}_i & \underline{t}'_i\end{bmatrix},\quad i=1,2\ . \tag{4.1}$$

The $\underline{S}$ matrix is unitary: $\underline{S}_i^{\dagger}\underline{S}_i=\underline{I}$, $S_iS_i^{\dagger}=\underline{I}$ (the unit matrix in the appropriate space). Time-reversal invariance implies the relation $t_i(m,n)=t'_i(n,m)$ and the symmetry of the matrices $\underline{r}_i$ and $\underline{r}'_i$.

The transmission and reflection amplitudes pertaining to the combined system are $\underline{t}_{12}$, $\underline{r}_{12}$, $\underline{t}'_{12}$, and $\underline{r}'_{12}$. Our task is then to express these four amplitudes in terms of the amplitudes of the individual channels. Let us start with t_{12}. The transmission of the combined system can be computed as the coherent sum of all waves traveling and bouncing between the two barriers. This series of waves can be arranged according to an increasing number of internal reflections between barriers 1 and 2.

We will use matrix multiplication corresponding to a propagation of the wave between barriers 1 and 2. For the single-channel case, the amplitudes are c numbers and the order in which they appear is not important. In the multichannel case, the amplitudes are matrices and the order is crucial. We have above adopted the convention that a matrix element t_{mn} is the transmission amplitude for the outgoing wave of mode m due to an incoming wave of mode n. With this convention the order of amplitudes in any product is opposite to what appears in the schematic description in terms of successive scattering events.

The first term in the multiple-scattering series for t_{12} represents a wave which just goes through the two barriers without any reflection and gives the contribution $\underline{t}_2\underline{t}_1$ to $\underline{t}_{12}$. The second term consists of the following events: (1) transmission through barrier 1 with amplitude $\underline{t}_1$; (2) reflection from the left on barrier 2 with amplitude $\underline{r}_2$; (3) reflection from the right on barrier 1 with amplitude $\underline{r}'_1$; (4) transmission through barrier 2 from left to right with amplitude $\underline{t}_2$. Combining all four steps, the contribution of the second term to $\underline{t}_{12}$ is $\underline{t}_2\underline{r}'_1\underline{r}_2\underline{t}_1$. It is now easy to deduce the contribution of the next term, which is simply $\underline{t}_2(\underline{r}'_1\underline{r}_2)^2\underline{t}_1$ and so on. The contribution from the infinite series is evaluated as a geometrical progression with the result $\underline{t}_{12}=\underline{t}_2(1-\underline{r}'_1\underline{r}_2)^{-1}\underline{t}_1$. Similar relations hold for $\underline{r}_{12}$, $\underline{t}'_{12}$, and $\underline{r}'_{12}$. These relations are given explicitly as

$$\underline{t}_{12}=\underline{t}_2(1-\underline{r}'_1\underline{r}_2)^{-1}\underline{t}_1\ , \tag{4.2a}$$

$$\underline{r}_{12}=\underline{r}_1+\underline{t}'_1\underline{r}_2(1-\underline{r}'_1\underline{r}_2)^{-1}\underline{t}_1\ , \tag{4.2b}$$

$$\underline{t}'_{12}=\underline{t}'_1(1-\underline{r}_2\underline{r}'_1)^{-1}\underline{t}'_2\ , \tag{4.2c}$$

$$\underline{r}'_{12}=\underline{r}'_2+\underline{t}_2\underline{r}'_1(1-\underline{r}_2\underline{r}'_1\underline{1})^{-1}\underline{t}'_2\ . \tag{4.2d}$$

Equations (4.2) still hold, even when the transmission matrices are not square, corresponding to the case in which the number of incoming channels is different from the number of outgoing channels (the reflection matrices are always square). This is one of the advantages of the present method compared with the usual transfer-matrix approach. In terms of the $\underline{S}$ matrices, we then write

$$\underline{S}_{12}=\underline{S}_1*\underline{S}_2\ , \tag{4.3}$$

where the star-product operation defined through Eqs. (4.2) has been applied by Redheffer in the theory of waveguides.[22] It is then possible to add the barriers one after the other until the entire system is worked out. The unitarity bound on the reflection and transmission matrices assures the existence of the inverse $(\underline{1}-\underline{r}'_1\underline{r}_2)^{-1}$ and guarantees the convergence of the procedure for any number of steps. It is worth mentioning here that if the barriers are infinitesimally close to each other, the star product is transformed into a nonlinear differential relation, which eventually leads to a matrix Riccati equation for the reflection amplitudes.

From a practical point of view, it appears that the most economic way is to use Eq. (4.2d). If one includes under barrier 1 the collection of L barriers whose

reflection amplitude from the right has already been calculated, and barrier 2 is a new one added to the right of these L barriers, then only Eq. (4.2d) has to be employed. Once $\underline{r}'_{12}$ is computed, the total transmission coefficient $\underline{t}'_{12}\underline{t}'^{\dagger}_{12}$ is evaluated from the total reflection $\underline{r}'_{12}\underline{r}'^{\dagger}_{12}$ through the unitarity relation.

B. Random-link model

Although this paper is mainly concerned with the percolating (missing-link) model, it will be useful to present also the numerical algorithm for the random-link model. In this case all the links are present, but the wave number on each link is random. In order to include also the effect of tunneling, the disorder is introduced as link potentials v_j, giving rise to the wave number of the link $\kappa_j=(k^2-v_j)^{1/2}$. In Sec. IV A we have explained how the transmission of individual units is combined to give the transmission of the whole system. Now we have to explain what the pertinent units are and how the transmission and reflection through each unit is computed. The illustration will be carried out on the two-dimensional lattice, but the extension to a three-dimensional lattice presents no difficulty.

Transmission and reflection occur at each column of sites followed by the accumulation of phases as the wave propagates between two such columns. Thus each unit consists of a column of sites together with the links located on its right side (see Fig. 8). In order to evaluate the transmission and reflection at a given column of sites, we number the sites from 1 to N and consider a site m ($m=1,2,\ldots,N$). The wave number to its left is k_m, while the wave number to its right is p_m. The wave numbers in the transverse direction are q_m (above the site) and q_{m-1} (below the site). We adopt here periodic-transverse-boundary conditions so that $q_0=q_N$. On a transverse link between sites m and $m+1$, the wave function is given by

$$\psi(y)=c_m e^{iq_m y}+d_m e^{-iq_m y} , \tag{4.4}$$

where the coordinate y is measured from link m.

An incoming wave of unit amplitude reaching site n from the left will provoke, in any site m, leftward reflected waves with reflection amplitude r_{mn}, as well as rightward transmitted waves with transmission amplitude t_{mn}. The matching equations [Eqs. (2.4)–(2.6)] now imply the following relations (the dependence of the transverse coefficients c and d on the incoming index n will not be indicated; the lattice spacing is denoted by a as before):

$$\delta_{mn}+r_{mn}=t_{mn}=c_m+d_m=c_{m-1}e^{iq_{m-1}a}+d_{m-1}e^{-iq_{m-1}a} , \tag{4.5}$$

$$k_m(\delta_{mn}-r_{mn})+q_{m-1}(c_{m-1}e^{iq_{m-1}a}-d_{m-1}e^{-iq_{m-1}a}) =p_m t_{mn}+q_m(c_m-a_m) ,$$

where δ_{mn} is the Kronecker delta function. The equality $\delta_{mn}+r_{mn}=t_{mn}$ results simply since reflection and transmission occur at the same point in space. From the first set of equations in (4.5), one can now eliminate the coefficients of the transverse motions pair by pair using the relations

$$c_m+d_m=t_{mn},\quad c_m e^{iq_m a}+d_m e^{-iq_m a}=t_{m+1,n} . \tag{4.6}$$

We now substitute the solution of Eqs. (4.6) into the second set of equations in (4.5) and replace r_{mn} by $t_{mn}-\delta_{mn}$. As a result, we get a set of equations for the transmission matrix $\underline{t}=\{\underline{t}_{mn}\}$ of the pertinent site of columns, which reads

$$\underline{A}t=2\underline{K} , \tag{4.7}$$

where the $N\times N$ matrices $\underline{A}$ and $\underline{K}$ are given by

$$\begin{aligned}
&\underline{A}(m,m)=k_m+p_m+i[q_m\cot(q_m a)+q_{m-1}\cot(q_{m-1}a)] ,\\
&\underline{A}(m,m+1)=-iq_m\csc(q_m a) ,\\
&\underline{A}(m,m-1)=-iq_{m-1}\csc(q_{m-1}a) ,\\
&\underline{K}=\mathrm{diag}(k_1,k_2,\ldots,k_N) ,
\end{aligned} \tag{4.8}$$

with $m=1,2,\ldots,N$ and $N+1$ or 0 are defined mod N. The solution of Eq. (4.7) yields the transmission matrix from left to right, and then the corresponding left to left reflection matrix $\underline{r}=\underline{t}-\underline{I}_N$ ($\underline{I}_N$ is the unit matrix) is obtained. To get the matrices pertaining to waves approaching from the right, one has to interchange the roles of k_m and p_m. Since the matrix $\underline{A}$ is not affected by this swap, it does not require any additional matrix-inversion procedure.

It is worthwhile noting here that in the presence of a constant magnetic field perpendicular to the direction of propagation, the only change in the above formalism concerns the nondiagonal elements of the matrix A. If the columns of sites are numbered as $1,2,\ldots,L$, and the magnetic flux per plaquette is ϕ ($\phi=Ba^2$ in units of hc/e), then at column l ($l=1,2,\ldots,L$) one has

$$\begin{aligned}
&\underline{A}(m,m+1)\rightarrow\underline{A}(m,m+1)e^{2\pi il\phi} ,\\
&\underline{A}(m,m-1)\rightarrow\underline{A}(m,m-1)e^{-2\pi il\phi} .
\end{aligned} \tag{4.9}$$

These phases are identical to those multiplying the hopping integrals (the Peierls substitution) used, e.g., in tight-binding models.

What is left in order to complete the calculations of the individual unit shown in Fig. 8 is to take account of the

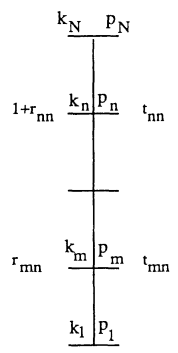

FIG. 8. Typical unit (column of sites) of a disordered lattice of wires.

phase between two units. This is easily accomplished using the matrix $P=\mathrm{diag}(p_1,p_2,\ldots,p_N)$ and the substitutions

$$\underline{t}\rightarrow e^{i\underline{P}}\underline{t},\quad \underline{r}\rightarrow\underline{r},\quad \underline{t}'\rightarrow\underline{t}e^{i\underline{P}},\quad \underline{r}'\rightarrow e^{i\underline{P}}\underline{r}'e^{i\underline{P}}\ . \tag{4.10}$$

We have thus explained how to evaluate the transmission and reflection amplitudes for each individual unit in the random-link model. Together with the composition law explained in Sec. IV A, we have at hand an algorithm for a numerical study of the full system. We repeat here that our approach will mostly be used in three dimensions, for which the relevant equations are slightly more complicated.

C. Percolating network

Unlike the former case in which all links are present, we will now study the case where part of the links are missing, while the others have a fixed wave number k. Such a lattice is schematically shown in Fig. 9. Within this figure a typical unit is shown (enclosed in a dashed rectangle), which is obtained by removing links from a complete unit discussed in connection with Fig. 8. In particular, the number of entrance channels, N_i, is different from the number of exit channels, N_f. Furthermore, the unit may be cut off at several points.

Before explaining how to evaluate the transmission and reflection amplitudes in this case, it is worthwhile mentioning that the transfer-matrix algorithm is ill defined in this context. To illustrate it let us consider (Fig. 10) a fork-shaped configuration where there is one incoming and two outgoing channels. In the transfer-matrix algorithm, each link is characterized by two coefficients and one is required to express the four coefficients pertaining to the two outgoing channels in terms of the two coefficients belonging to the initial channel. There are, however, only three matching equations at the vertex, which are not sufficient for this purpose. On the other hand, in the transmission reflection formalism adopted here, the incoming channel has an incoming wave of unit amplitude and an outgoing reflected wave with an unknown reflection coefficient, while each of the outgoing channels has an outgoing wave whose transmission amplitude is unknown. These three unknowns are completely determined by the three matching equations.

It is possible to obtain the amplitudes of our unit in the missing-link system as a special limiting procedure on the matrix $\underline{A}$ defined by Eqs. (4.8). If a transverse link m is missing, the coupling term involving q_m is omitted from the matrix $\underline{A}$. In this way each subunit is decoupled from the others. Note, however, that reflection from dead ends in the transverse direction is not neglected. If a longitudinal link n is missing on the left, this channel is missing from the calculations at this specific step. If a link m is missing on the right, we put $p_m=0$ in the corresponding diagonal element of $\underline{A}$. This procedure will guarantee in particular a correct treatment of the following two situations: (1) In case all the transverse links are also missing, the system reaches a longitudinal dead end and the reflection is complete with a phase equal to one; (2) in case some of the transverse links are present, the wave propagates as if the missing link did not exist. Note that if we require complete reflection with phase -1, then property (2) above will not be fulfilled. The size of the matrix $\underline{A}$ is equal to the number of occupied links on the left side of the unit. After Eqs. (4.7) are solved, the reflection matrices are computed simply by subtracting the unit matrix from the transmission matrices. Then the elements t_{mn} for which the link m is missing on the right are thrown away. The resulting square reflection matrices and the (not necessarily square) transmission matrices enter the calculations of the full system using the composition law Eq. (4.2).

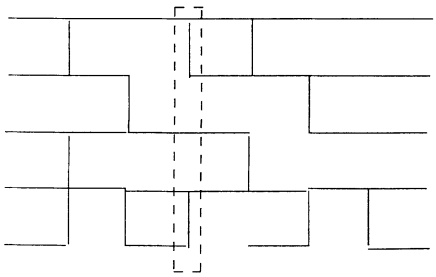

FIG. 9. Percolating lattice of wires with a typical unit.

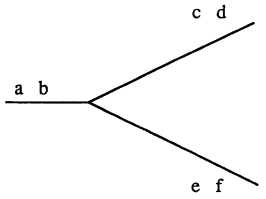

FIG. 10. Fork-shaped intersection of wires which cannot be described by a transfer matrix.

V. RESULTS FOR THE DISORDERED SYSTEM

A. Quantum-percolation threshold p_q and critical exponent ν

In this section we will demonstrate that the model presented above exhibits a bona fide percolation transition in three dimensions, while there is no such transition in two dimensions. We stress here that the calculations presented below do not pretend at being very accurate as far as several digits and error-bar determination of the exponents and threshold probability is concerned. Rather, they intend to provide a quantitative global picture of the problem.

Our arguments are mainly based on numerical calculations pertaining to a three-dimensional cube or a two-dimensional square of side La. Actually, the lattice constant a enters only through the dimensionless parameter ka, where k is the Fermi momentum and the electron's energy is simply equal to k^2. In the thermodynamic limit, the occupation probability p and $ka\ (\mathrm{mod}\,\pi)$ are the only relevant parameters. For finite-size samples, the system size L is an additional parameter. We recall that if L is finite, the quantum-mechanical conductance g has some probability distribution. If L is infinite, the conduc-

tance (away from p_q) is self-averaging. The localization length ξ can be expected to be the relevant crossover length for the self-averaging behavior.

Our first task is to find out whether the model presented above exhibits a phase transition in three dimensions and to decide whether this transition is a percolation transition. If the answer is positive, we can continue and determine the scaling behavior of the conductance as well as the critical exponents. As we have explained in the Introduction, it is expected that the critical probability p_q for the quantum-mechanical system will be larger than the corresponding classical quantity $p_c=0.248\,812$ (see Ref. 2) as a result of localization. Furthermore, the critical probability is not a universal quantity and is then expected to be energy dependent. At the same time we want to show that, according to the scaling theory of localization, there is no Anderson transition in two dimensions. We now explain three methods for studying the critical behavior if it exists.

The most naive way by which p_q may be estimated would consist in plotting the quantity $-\ln(\langle g\rangle)$ as a function of $\ln(L)$ for several values of the occupation probability p [up to a sign, this function is the primitive of the celebrated renormalization-group scaling function $\beta(g)$]. If an insulator-conductor transition exists for $d=3$, it should show up as a sign change of the scaling function $\beta(g)=d[\ln(\langle g\rangle)]/d[\ln(L)]$. Thus, for $p<p_q$, we expect the function $-\ln(\langle g\rangle)$ to have a positive slope, while for $p>p_q$ the slope should be negative. For $d=2$, however, we expect all the lines to have a positive slope except near $p=1$, where a crossover to the ordered case occurs.

Second, we may borrow the finite-size-scaling argument for the conductivity of the classical network. We recall from Eq. (1.1) that for a cube of side L in d dimensions the mean classical conductivity $\Sigma_L(p)$ is expected to behave in the critical region ($|\Delta|=|p-p_q|$ very small and L large) as $\Sigma_L(p)\approx L^{-t/\nu}F(\Delta L^{1/\nu})$, where F is a scaling function. Relating the conductivity Σ_L to the conductance $\langle g_L\rangle$ as $\Sigma_L=\langle g_L\rangle/L^{d-2}$, we get (under these special conditions) the following behavior of the mean quantum-mechanical conductance in the critical region:

$$\langle g_L(p)\rangle\approx L^{d-2-t/\nu}F(\Delta L^{1/\nu})\ , \tag{5.1}$$

where the scaling function F and the critical exponent ν are, of course, different from their classical analogs. We recall that unlike the classical situation in $d=3$, the equality $t=\nu$ is predicted by nonlinear σ models. However, we can locate the critical quantum probability p_q even without knowing t or ν (or relying on the equality $t=\nu$) by noticing that in computing the ratio $\gamma(p)\equiv \mathrm{Var}(g)/\langle g\rangle^2$ between the variance and square of the average of the conductance g, the prefactors multiplying the scaling function F cancel, and hence, near the percolation threshold, we have

$$\gamma_L(p)=\frac{\mathrm{Var}(g)}{\langle g\rangle^2}=\frac{\langle g^2\rangle}{\langle g\rangle^2}-1\approx H(\Delta L^{1/\nu})\ , \tag{5.2}$$

where H is another scaling function. Thus all graphs of $\gamma_L(p)$ as a function of p for different values of L should meet at the same point $p=p_q$ corresponding to $H(0)$. Using relation (5.2) slightly away from the percolation threshold will enable us to estimate the critical exponent ν and [through relation (5.1)] test the prediction $t=\nu$.

Finally, if the equality $t=\nu$ is adopted at the outset, we see from Eq. (5.1) that the prefactor of the scaling function F disappears for $d=3$. Hence, if the quantum-mechanical conductance $g_L(p)$ undergoes a percolating transition at $p=p_q$, all the quantities $\langle g_L(p)\rangle$ for different values of L should cross each other at $p=p_q$. Furthermore, since the percolation transition is also an Anderson transition, we expect $\langle g_L(p)\rangle$ to decay exponentially with L for $p<p_q$ and to increase as L for $p>p_q$. In other words, the slope $d[\langle g_L(p)\rangle]/dp$ at $p=p_q$ is positive and must grow with L. It follows from Eq. (5.1) that this quantity approximately equals $L^{1/\nu}F'(0)$ (for $t=\nu$) and hence $F'(0)>0$. A stringent test of the equality $t=\nu$ is therefore provided by a plot of some function of $\langle g_L(p)\rangle$ (say, $\ln[\langle g_L(p)\rangle]$) for several values of the parameter $x=\Delta L^{1/\nu}$. With an educated guess of p_q and ν, all the points must fall on a smooth curve, which is the graph of $\ln[F(x)]$.

We are now in a position to analyze our results pertaining to the critical probability p_q as well as the critical exponents t and ν. Some information concerning our numerical computations is in order. The discussion in Sec. IV implies that the size of the matrices involved is L^2 and the number of operations is proportional to L. Thus the computing time grows very fast with the system size. We have generated an ensemble of at least several hundreds of samples for each value of p and L. For $d=3$ the maximal system size was $L=10$; namely, we had to perform operations on complex matrices of dimension up to 100. Each realization of a $10\times10\times10$ cube required about 4 s on a Cray 1 computer. It is also reasonable to limit the lattice side from below at $L=4$, say. For $d=2$ the length L can assume much higher values.

It has already been shown that the pure system ($p=1$) has a band for $0\le k\le\pi$, which is symmetric about $\pi/2$. Our main results are presented for k at the band center (actually, we shift it slightly to avoid dealing with a rational multiple of π). Later on, we will discuss the dependence of p_q on energy (in this special investigation, the value of k will, of course, be varied).

Starting with the dependence of $\ln(\langle g\rangle)$ on $\ln(L)$, we begin by demonstrating the absence of an Anderson transition in $d=2$ and plot in Fig. 11 the function $-\ln(\langle g\rangle)$ as a function of $\ln(L)$ pertaining to squares of length $L=8-22$ for p between 0.75 and 1. For $p<0.9$ all the lines have positive asymptotic slope, and therefore they correspond to a negative β function, as expected for Anderson insulators. For $p=0.9$ the slope is close to zero. Since we know that for $p=1$ (an ordered crystal) the slope is exactly -1, we interpret the zero slope at $p=0.9$ as a finite-size correction. In other words, the slope is negative as long as we remain in the (quasi)metallic regime $L<\xi$, but we expect it to be positive once we cross into the insulating regime as L increases further. As p approaches 1, we are tempted to describe the crossover

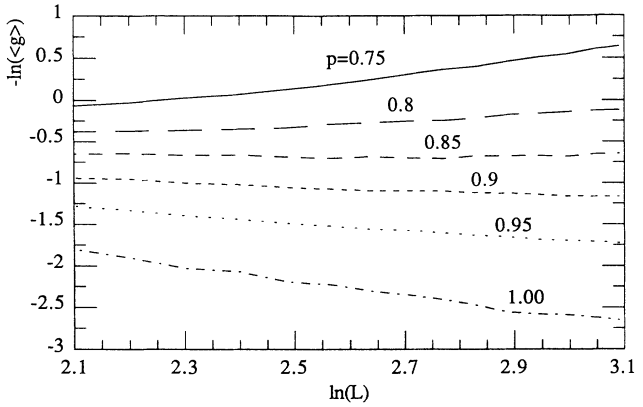

FIG. 11. (a) Quantity $-\ln\langle g\rangle$ vs $\ln(L)$ for a two-dimensional percolating lattice of wires for p between 0.75 and 1.

between the (quasi)metallic and ballistic regimes by the scaling formula

$$\frac{\langle g_L(p)\rangle}{L}=U((1-p)L)) \quad (d=2,\ L\gg 1,\ 1-p\ll 1)\ , \tag{5.3}$$

where $U(0)$ is a constant (see Sec. III) and $U(x)$ $[x=(1-p)L]$ vanishes roughly as $1/x$ as x tends to infinity. One can justify Eq. (5.3) by noting that $(1-p)^{-1}$ is proportional to a typical distance l between missing bonds, and hence the argument of the scaling function U is $x=L/l$. The quantity $\langle g_L(p)\rangle/L$ is plotted as a function of x in Fig. 12. Actually, one expects an exponential decay of the conductance for $L\gg\xi$ (as discussed already in connection with Fig. 11), but this behavior cannot be seen from the numerical data, confirming thus that ξ blows up very rapidly as $p\to 1$. We recall that nonlinear σ models predict an essential singularity $\xi\sim\exp[c/(1-p)]$ for some positive constant c. The crossover between the metallic and ballistic regimes for $d=3$ (which will be discussed in Sec. V C) is easier to grasp, since in $d=3$ there is only one length scale l, while in $d=2$ there are two length scales l and ξ.

Having thus confirmed the absence of a transition in $d=2$, we now move on to study the three-dimensional (3D) system. It has been found useful to take the classical percolation threshold $p_c\approx 0.25$ as a reference point. The quantity $-\ln(\langle g\rangle)$ as a function of $\ln(L)$ is plotted in Fig. 13 for five values of $p-p_c$, namely, $p-p_c=0.05$, 0.15, 0.25, 0.35, and 0.45. It is immediately verified that the first two lines (pertaining to $p-p_c=0.05$ and 0.15) have a positive slope, and hence they correspond to a negative value of the scaling function $\beta(g)$. Therefore, at least up to $p=p_c+0.15=0.40$, the system is an insulator in the Anderson sense. On the other hand, the slope of the last three lines (pertaining to $p-p_c=0.25$, 0.35, and 0.45) is positive, so that they correspond to a positive value of the scaling function $\beta(g)$. We can therefore conclude that, at least down to $p=p_c+0.25=0.50$, the system is a conductor in the Anderson sense. Consequently, the system undergoes an Anderson transition, as expected for $d=3$. The parameter $q=1-p$ can be considered in some sense as the strength of the disorder (a role played by the parameter W in the standard Anderson model) and the transition occurs for $0.4<p<0.5$. Instead of studying this transition through the divergence of the localization length, we prefer to draw the analogy with the classical percolation transition. Yet it should be stressed that, as far as the physics is concerned, the basic ingredient is the standard Anderson transition.

Let us first analyze our results within the finite-size-scaling hypothesis (5.1), but without relying on the assumption $t=\nu$. In particular, this analysis will enable us to deduce the value of both p_q and ν in a consistent manner. In this context we first plot in Fig. 14 the function $\gamma_L(p)$ [defined in Eq. (5.2)] of our 3D $L\times L\times L$ bond percolating lattice of wires for $L=5$, 6, 7, 8, and 10. We remark that all functions nearly coincide for $p-p_c=0.20\pm 0.02$. Thus the fact that the present transition is a percolation transition with a critical probability p_q near 0.45 is now established within the finite-size-scaling hypothesis (5.1). Note the strong variation of the function $\gamma_L(p)$ in a narrow range of p around the threshold. This is related to an abrupt change in the whole distribution of the conductance, as will be discussed later on. Since the scaling form expressed in Eq. (5.2) holds in the vicinity of the threshold, we can use it to find both p_q

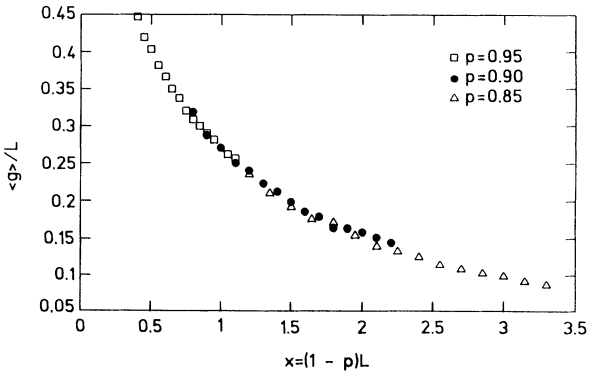

FIG. 12. Function $\langle g\rangle/L$ (for a two-dimensional percolating lattice of wires) as a function of the scaling variable $x=L(1-p)$ for p close to 1.

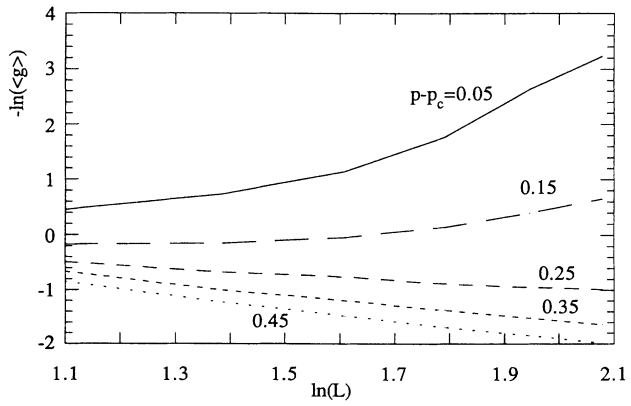

FIG. 13. Quantity $-\ln\langle g\rangle$ vs $\ln(L)$ for a three-dimensional percolating lattice of wires for $p-p_c$ between 0.05 and 0.45 supporting the claim on the presence of transition in $d=3$.

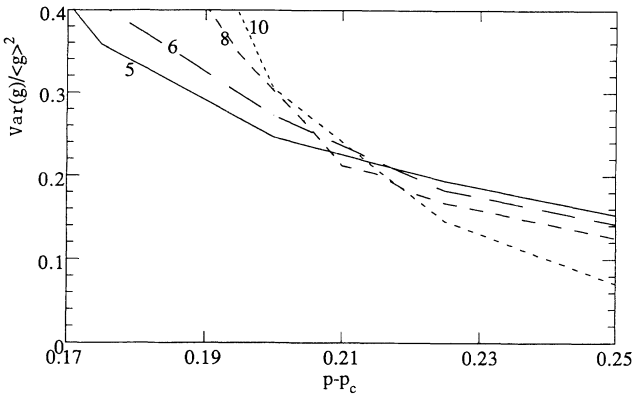

FIG. 14. Ratio $\mathrm{Var}(g)/\langle g\rangle^2$ for a three-dimensional percolating lattice of wires as a function of $p-p_c$ for $L=5$, 6, 7, 8, and 10, indicating the existence of a quantum transition based on the finite-size-scaling hypothesis without relying on the equality $t=\nu$.

and ν. This can be done directly by noticing the relation $d\gamma_L/dp=L^{1/\nu}H'(0)$ at $p=p_q$, so that a plot of $\ln(d\gamma_L/dp)$ vs $\ln(L)$ should have a slope $1/\nu$. Unfortunately, the error bar on p_q and the need to compute numerical derivatives make this approach impractical. The procedure we adopt is to guess values for both p_q and ν and to plot $\ln[\gamma_L(p)]$ for all available values of the argument $x=\Delta L^{1/\nu}$. If the choice of p_q and ν is correct, then a plot of the values of $\ln[\gamma_L(p)]$ corresponding to the respective points x should fall on a smooth curve which represents the scaling function $\ln[H(x)]$ appearing on the right-hand side of Eq. (5.2). In fact, we have already established an approximate value of p_q, and so we may fix it at 0.45 and concentrate on the value of ν. Figure 15(a) is an (intentionally unsuccessful) attempt to trace the scaling function $\ln[H(x)]$ for $p_q=0.45$ and $\nu=0.5$, while Fig. 15(b) is a much better attempt with $p_q=0.45$ and $\nu=0.75$. From this analysis we may again conclude that $p_q=0.45\pm0.02$ and $\nu=0.75\pm0.1$ (see our remarks concerning error bars and accuracy at the beginning of this section). Any deviation from these values beyond reasonable error bars strongly reduces the success of the fit, as we may judge from the difference between Figs. 15(a) and 15(b). The value of the critical exponent $\nu=0.75$ is consistent with a rigorous bound by Chayes *et al.*[25] that predicts the relation $d\nu>2$ for random systems. Note that the value of ν found here is smaller than the classical value in 3D geometrical percolation,[2] which is equal to 0.875. It is much smaller than the numerical value ($\nu=1-1.5$) often found[26] for the Anderson model.

We now analyze our results according to the finite-size-scaling hypothesis [Eq. (5.1)], but this time we take the equality $t=\nu$ as given from the onset. This leads in $d=3$ dimensions near p_q to the relation $\langle g_L(p)\rangle \approx F(\Delta L^{1/\nu})$. In Fig. 16 we plot the average conductance $\langle g_L(p)\rangle$ of our 3D $L\times L\times L$ bond percolating lattice of wires for $L=5$, 6, 7, 8, and 10. It has been demonstrated in the previous discussion that the relevant domain for the probability p (as far as the critical value p_q is concerned) is $0.4<p<0.5$, namely, $0.15<p-p_c<0.25$. The behavior of the conductance at higher values of p will be discussed separately.

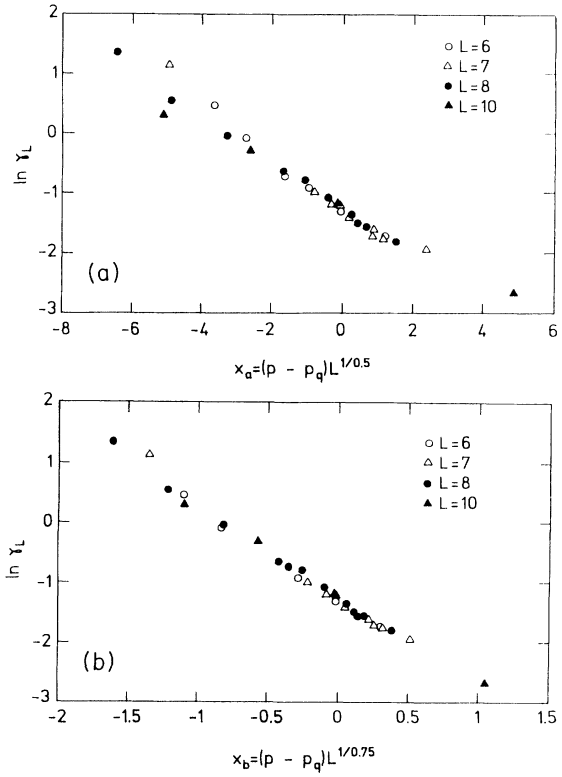

FIG. 15. (a) Quantity $\ln[\gamma L(p)]$ for a three-dimensional percolating lattice of wires as a function of the scaling parameter $x=(p-p_q)L^{1/\nu}$, displaying the scaling function $\ln[H(x)]$ for $p_q=0.45$ and $\nu=0.5$ (poor fit). (b) Same as (a) with $\nu=0.75$ (better fit).

It is evident from Fig. 16 that the functions $\langle g_L(p)\rangle$ for the five different values of L nearly coincide for $p-p_c=0.20\pm0.01$. This result indicates that within the finite-size-scaling hypothesis with $t=\nu$ the present transition is indeed a percolation transition with a threshold probability p_q near 0.45. Note also that the derivative $d[\langle g_L(p)\rangle]/dp$ at $p=p_q$ is positive and grows with L, as

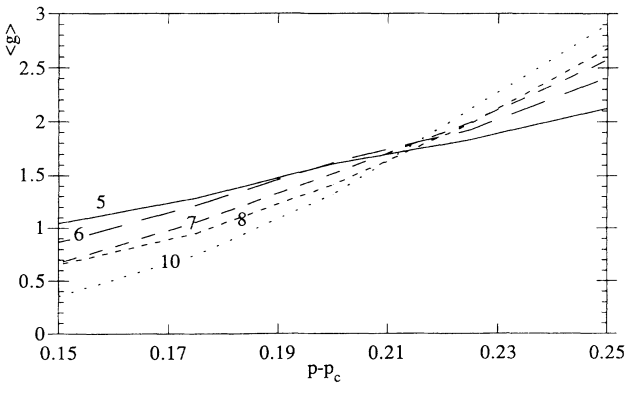

FIG. 16. Averaged conductance $\langle g\rangle$ for a three-dimensional percolating lattice of wires as a function of $p-p_c$ for $L=5$, 6, 7, 8, and 10, indicating the existence of a quantum transition based on the finite-size-scaling hypothesis and equality $t=\nu$.

expected for an Anderson transition. As indicated in connection with Fig. 1, the value of the quantum-mechanical threshold is indeed much higher than the classical value $p_c \approx 0.25$. The numerical estimate of p_q evaluated above is also much higher than the value 0.33 found by Meir, Aharony, and Harris[9] in some version of the Anderson model adapted for the study of quantum percolation. As we have already stated, the value of p_q is not universal and depends on energy. The behavior of p_q as a function of energy will be studied later on. Here we just indicate that for energies near the center of the band (for which our calculations are performed), the value of p_q is found to be exceptionally high.

To further employ the finite-size-scaling hypothesis (5.1) with the assumption $t=\nu$, we suggest the value $p_q=0.45$ for the critical probability and $\nu=0.75$ for the critical exponent and plot in Fig. 17 the quantity $\ln[\langle g_L(p)\rangle]$ for several values of the parameter $x=\Delta L^{1/\nu}$. As we can judge, the points fall on a smooth curve, which, as we have asserted, is the graph of $\ln[F(x)]$, where $F(x)$ is the scaling function appearing in Eq. (5.1).

At this point it is of interest to relate the value of the critical exponent found here ($\nu=0.75$) to the result of Meir, Aharony, and Harris[9] regarding the size dependence of a quantity $[T(r,E)]$ defined as the average transmission of a wave with energy E between two points, a distance r apart. Using an entirely different model (a binary form of the Anderson model), they have found the behavior $[T(r,E)]\sim r^x e^{-r/\xi(E)}$, where $\xi(E)$ is the localization length and x is a critical exponent. They have investigated the series for the transmission coefficient and concluded that it behaves near threshold like $[\xi(E)]^{x+d}$. To get a numerical value for x, they have looked for a singularity of the form $|\Delta|^{-\gamma}$. Since the localization length diverges as $\Delta^{-\nu}$, one has $\gamma=\nu(x+d)$. In three dimensions they report the numerical estimate $\gamma\approx 0.5$. To test if this result is consistent with our estimate of ν, we recall that the conductance of a cube of length L in d dimensions is proportional to $L^{2(d-1)}[T(r,E)]^2$, which, at the percolation threshold $[\xi(E)\to\infty]$, is proportional to $L^{2(d-1)+2x}$. On the other hand, the finite-size-scaling argument leads, at the percolation threshold, to a conductance proportional to $L^{d-2-t/\nu}$ (the proportionality constant is irrelevant here). Thus we get $x=-\frac{1}{2}(d+t/\nu)$, which, for $d=3$ and $t=\nu$, gives $x=-2$. This yields $\gamma=\nu(x+d)=0.75$ compared with 0.5 reported by Meir, Aharony, and Harris. Given the fact that the two models and numerical procedures are entirely different, the two results for γ are comparable.

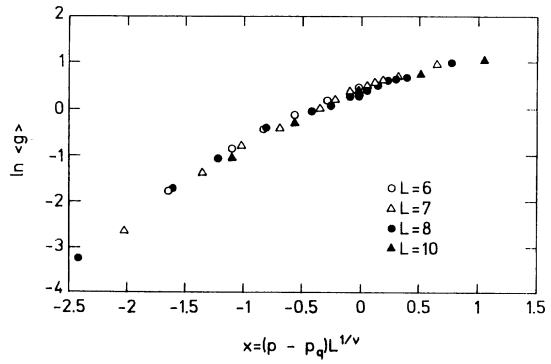

FIG. 17. Quantity $\ln(\langle g\rangle)$ for a three-dimensional percolating lattice of wires as a function of the scaling parameter $x=(p-p_q)L^{1/\nu}$ with $p_q=0.45$ and $\nu=0.75$. For $t=\nu$ the plot displays the scaling function $\ln[F(x)]$.

B. Energy dependence of the quantum-percolation threshold p_q

So far, we have limited ourselves to the center of the band $k=\pi/2$. At this energy we concluded that the critical occupation probability p_q is about 0.45. It is also expected that at the end of the band near $k=0$ the quantum-mechanical threshold approaches the classical one, that is, $p_q=p_c$. Indeed, if k is very small, the phase of the wave function is almost zero and the matching conditions at the sites coincide with those of the classical Kirchoff laws. To study the energy dependence of p_q for k between 0 and $\pi/2$, we used the procedure developed in connection with Eq. (5.2); namely, for a fixed value of k we looked for the common intersection of all the curves $\gamma_L(p)$. The intersection point has been taken as our evaluation of the energy-dependent threshold p_q. Since our main goal here is to get a rough estimate, we have first limited ourselves to four values of L, namely $L=4$, 5, 6, and 7, and evaluated $p_q(k)$ for $k=\pi/6$, $\pi/3$, and $6\pi/13$. Later on, we added the points $\pi/13$ and $\pi/4$ based on calculations with $L=6$ and 8. Together with the values available at the end of the band at $k=0$ and at the middle of the band at $k=\pi/2$, we can get a clear global picture. This is demonstrated in Fig. 18. From this figure we see in particular that the value of p_q at the center of the band is maximal.

C. Behavior of the conductance in the metallic regime ($p>p_q$)

The following discussion is not directly related to the investigation of the electrical conductance at the percolation threshold, but for the sake of completeness we find it useful to study the behavior of the conductance at $p>p_q$. For large values of the occupation probability ($p\to 1$), we

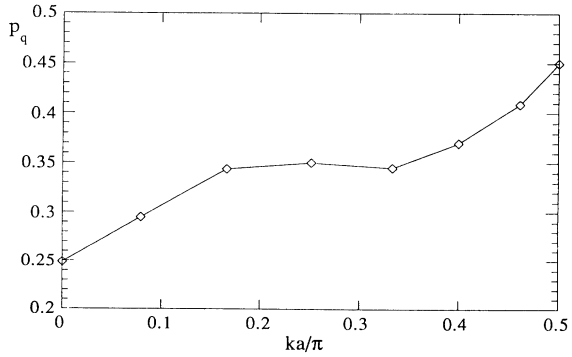

FIG. 18. Dependence of p_q on energy for a three-dimensional percolating lattice of wires (evaluated at eight points within the energy band). The solid curve is meant as a guide for the eye.

are in the weak disorder regime. From the discussion of Fig. 13 (related to the β function), we have seen that above threshold the slope of the function $-\ln(g)$ vs $\ln(L)$ is 1, so that for $p > p_q$ the conductance grows linearly with L in accordance with Ohm's law. It is also predicted by the diagrammatic approach to the Anderson localization problem in the weakly localized regime.[27] The crossover picture between the metallic and critical regimes in $d > 2$ is clear. The L^{d-2} behavior in the metallic regime is changed to an $L^{d-2-t/\nu}$ behavior as $p \to p_q$ from above, in accordance with the finite-size-scaling hypothesis. On the other hand, we have seen in Sec. III that for the perfect lattice ($p = 1$) the conductance is proportional to the number of channels, namely, L^{d-1}. Thus there is an additional crossover between the metallic and ballistic regimes.

As far as we know, the behavior of the conductance in the crossover region $p \to 1$ has not been investigated in detail so far. Most of the results derived from the scaling theory of the conductance in the weak disorder regime are applicable to any amount of disorder. Hence, in the thermodynamic limit, $p = 1$ must be a singular point. For finite size we expect the crossover between ballistic and diffusive regimes to be sharper and sharper as L increases. We demonstrate it in Fig. 19, in which we plot the conductance as a function of p in the domain $0.4 \le p \le 1$ for $L = 5-8$. At intermediate values of p, the conductance is linear, its value being proportional to L. As p approaches 1, the conductance grows at a higher power of p and the crossover region is smaller for larger L.

It is reasonable then to assume that the singularity at $p = 1$ in the thermodynamic limit is translated for a large but finite-size L (near $p = 1$) to a new scaling law of the form

$$\langle g_L(p) \rangle \approx L^2 K(L(1-p)) \quad (d = 3, L \gg 1, 1-p \ll 1) , \tag{5.4}$$

which is the analog of Eq. (5.3) for $d = 3$. The scaling function $K(y)$, $y = L(1-p)$, should behave like $1/y$ for large values of y in order to assure the L^{d-2} behavior of the conductance in the metallic (weakly localized) regime.

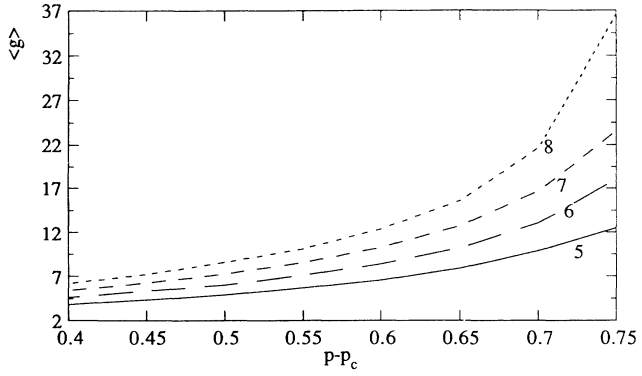

FIG. 19. Averaged conductance $\langle g \rangle$ for a three-dimensional percolating lattice of wires in the diffusive region $p_q < p < 1$ for $L = 5$, 6, 7, and 8, indicating the existence of a crossover domain between the diffusive and ballistic regimes.

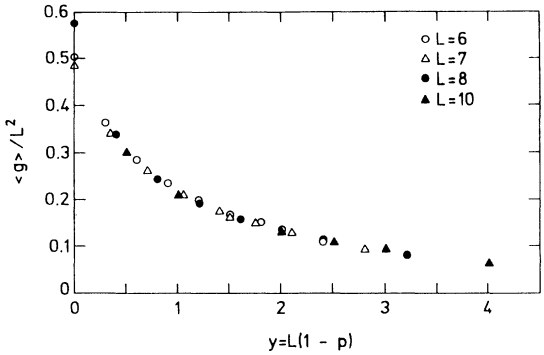

FIG. 20. Function $\langle g \rangle / L^2$ (for a three-dimensional percolating lattice of wires) as a function of the scaling variable $y = L(1-p)$ for p close to 1, displaying the scaling function $K(y)$ in Eq. (5.4).

On the other hand, the scaling function $K(y)$ must have a finite (nonzero) limit as $y \to 0$. This is indeed the case, as we can judge from a glance at Fig. 20, where we plot the quantity $\langle g_L(p) \rangle / L^2$ as a function of the scaling variable $y = L(1-p)$. Within reasonable error bars all the points lie on a smooth curve, which represents the scaling function $K(y)$. The finite limit as $y \to 0$ is manifest as well as the approximate behavior $K(y) \sim y^{-1}$ for large values of y. We have thus confirmed the occurrence of a sharp crossover between the diffusive and ballistic regimes in $d = 3$. Note that in $d = 2$ dimensions the situations looks identical, although there is, in principle, no diffusive regime, strictly speaking.

D. Distribution of the conductance in the neighborhood of the percolation threshold

There has been much interest in the distribution of the conductance in the metallic regime (where the disorder is weak) and in the insulating regime (where the disorder is strong). In the first case one of the most celebrated results is the occurrence of universal conductance fluctuations. Both the diagrammatic approach and random-matrix theory predict that in the metallic regime the transmission has a normal distribution whose variance is a universal number which depends only on the symmetry (universality class) and the dimension of the system (but rather weakly). In the second case the results are less definitive. Most investigations indicate that the conductance obeys a log-normal distribution, but the variance of $\ln(g)$ is not universal. The length dependence of $\mathrm{Var}[\ln(g)]$ has been studied recently using the method of directed paths. It is claimed in some recent works that $\mathrm{Var}[\ln(g)] \sim L^{\omega}$, where the exponent ω is universal and depends only on the dimension of the system.[28] It is also conjectured that in the insulating regime the two quantities $\mathrm{Var}[\ln(g)]$ and $-\langle \ln(g) \rangle$ are of the same order of magnitude. This can be checked explicitly in 1D, where g obeys a log-normal distribution[29] with $\langle \ln(g) \rangle \sim L$ and also $\mathrm{Var}[\ln(g)] \sim L$.

It is then of great interest to study the distribution of the conductance in the transition region, i.e., around

$p=p_q$. The results of this study are not universal, but they can indicate about the general trend. We can suspect that the distribution of the conductance at the percolation threshold becomes very wide. Therefore, we propose the following picture concerning the distribution of the conductance: (i) Below p_c we are in the insulating regime, neither $\langle g \rangle$ nor its variance are universal, and Var[ln(g)] is of the order of magnitude of $-\ln(g)$; (ii) at the percolating point, the variance is anomalously large (the conductance has a wide distribution); (iii) above the percolation threshold, we are in the metallic regime and the variance is a universal number of order 1. These predictions have already been manifested in connection with Fig. 14, where it is evident that the function $\gamma_L(p)$ [introduced in Eq. (5.2) as the ratio between the variance and the square of the averaged conductance] becomes very steep as a function of p around the percolation threshold.

A much better illustration can be presented by showing the distribution of the conductance itself [in the present model it is not practical to study the quantity $\langle \ln(g) \rangle$ for $p_c \leq p \leq p_q$ since for many samples the conductance is strictly zero because the system is cut off]. Figures 21(a)–21(e) display the distribution of the conductance below, at, and above the quantum-mechanical percolation threshold for a three-dimensional system of length $L=10$. The dramatic change between these three domains when p is varied on a relatively small scale is very convincing. The normal distribution above threshold and the wide distribution at threshold are very well reproduced.

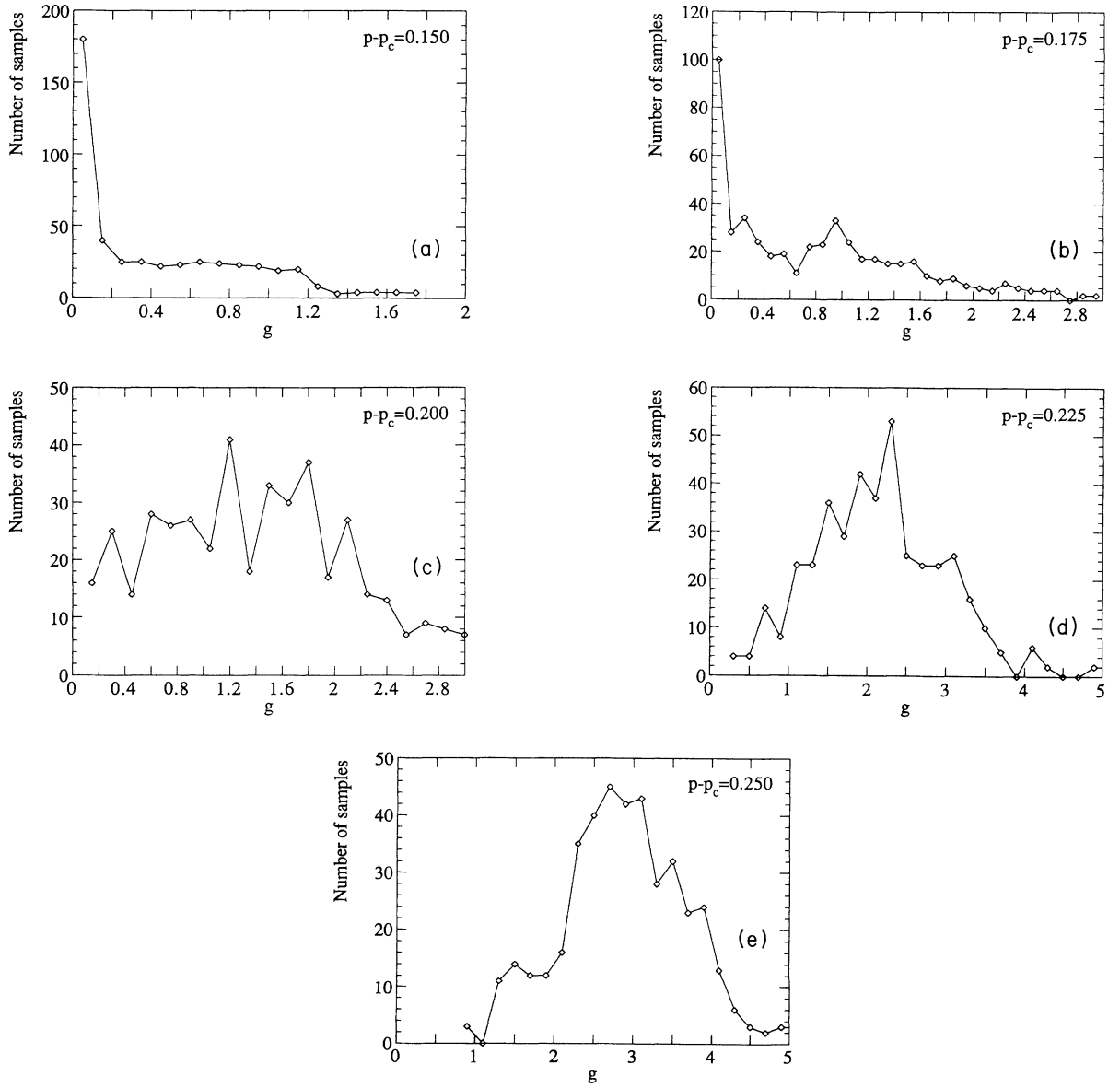

FIG. 21. (a) Distribution of the conductance for a three-dimensional percolating lattice of wires of length $L=10$ around $p=p_q$, showing the violent change in the variance and in the shape of the distribution. Here $p-p_q=-0.050$. (b) Same as (a) with $p-p_q=-0.025$. (c) Same as (a) with $p=p_q=0.450$. (d) Same as (a) with $p-p_q=0.025$. (e) Same as (a) with $p-p_q=0.050$.

VI. SUMMARY AND OPEN QUESTIONS

We have developed a model based on a lattice of quantum wires which is especially useful to study the percolation transition of the quantum-mechanical electrical conductance. Before investigating the disordered case, we presented nontrivial solutions for ordered systems. First, we have presented an analytic expression for the energy-dispersion relation. Second, we have evaluated in a closed form the transmission through a square or cubic sample, and through a Bethe lattice.

We have then studied the disordered (percolating) situation. It has been confirmed that there is no transition for $d=2$, while in $d=3$ dimensions there is an Anderson transition in which the probability $q=1-p$ plays the role of disorder strength. The quantum-mechanical threshold probability p_q is energy dependent, but always larger than the classical threshold p_c. At the center of the band, we have the estimated value $p_q=0.45\pm0.02$. The critical exponent ν has approximately been evaluated at 0.75 and the equality of the exponents t and ν for the quantum-mechanical conductance at $d=3$ has been confirmed. We have also analyzed the crossover between the quasimetallic and ballistic regimes in $d=2$ dimensions and between the metallic or diffusive and ballistic regimes in $d=3$ dimensions. In both cases we suggest a new finite-size-scaling law. The distribution of the conductance around the transition has been studied, and its variance undergoes a violent change at this point.

Interesting questions which deserve more attention are the following. (1) How these results are affected when a magnetic field is applied? Recent works by Pichard *et al.*[30] and Bouchaud[31] indicate that in the insulating regime the application of a weak magnetic field increases the localization length by a universal factor for quasi-one-dimensional systems or by a nonuniversal factor for bona fide two- and three-dimensional systems. The demonstration is based either on the transfer-matrix approach or on an analysis of the essential role played by close electron orbits. The application of a strong magnetic field on a two-dimensional electron gas in a disordered system leads to the quantum Hall effect. It is then of interest to find out what will be the response of a two-dimensional electron gas in a percolating system to the application of an external (constant and strong) magnetic field. (2) What will be the response of the system to an applied external ac field? In the classical case the dependence of the ac conductance on the frequency ω is of special significance. Its singularities in the complex $i\omega$ plane (particularly those with small negative real and zero imaginary parts) are related to the response of the system to an electrical pulse. These phenomena are shown[2] to be related to the concept of Lifshitz tails. It is hence very significant to find out whether Lifshitz tails[32] appear also in the quantum-mechanical ac conductance.

ACKNOWLEDGMENTS

One of us (Y. A.) would like to thank A. McKinnon, J. B. Pendry, and P. Bell for interesting discussions concerning the model of quantum wires. He would also like to thank C. Lhuillier, M. Moreau, and the Department of Theoretical Physics of Liquids at the University of Paris VI for their warm hospitality when part of this work has been done. J.M.L. acknowledges N. L. Balazs for a stimulating discussion on related problems. Both of us are grateful to J. L. Pichard for his comments and suggestions. This work was partially supported by a grant from the American Israeli Binational Science Foundation and partially by the Sherman Foundation for Joint British Israeli researches.

[1] D. Stauffer, *Introduction to Percolation Theory* (Taylor and Francis, London, 1985).
[2] J. P. Clerc, G. Giraud, J. M. Laugier, and J. M. Luck, Adv. Phys. **39**, 191 (1990).
[3] S. Alexander and R. Orbach, J. Phys. Lett. (Paris) **43**, L625 (1982).
[4] P. G. de Gennes, P. Lafore, and J. P. Millot, J. Phys. Chem. Solids **11**, 105 (1959); J. Phys. Radiat. **20**, 624 (1959).
[5] S. Kirkpatrick and T. P. Eggarter, Phys. Rev. B **6**, 3598 (1972).
[6] T. Odagaki, Solid State Commun. **33**, 861 (1980).
[7] R. Raghavan, Phys. Rev. B **29**, 748 (1984).
[8] Y. Shapir, A. Aharony, and A. B. Harris, Phys. Rev. Lett. **49**, 486 (1982).
[9] Y. Meir, A. Aharony, and A. B. Harris, Phys. Rev. Lett. **56**, 976 (1986); Europhys. Lett. **10**, 275 (1989).
[10] G. Deutscher, Y. Lévy, and B. Souillard, Europhys. Lett. **4**, 577 (1987).
[11] Y. Lévy and B. Souillard, Europhys. Lett. **4**, 233 (1987).
[12] L. J. Root and J. L. Skinner, J. Chem. Phys. **89**, 3279 (1988).
[13] J. Pimentel and S. L. A. de Queiroz, J. Phys. A **22**, L345 (1989).
[14] C. J. Lambert and G. D. Hughes, Phys. Rev. Lett. **66**, 1074 (1991).
[15] M. E. Fisher, in *Critical Phenomena,* Proceedings of the International School of Physics "Eurico Fermi," Course 51, Varenna, edited by M. S. Green (Academic, London, 1971), p. 1.
[16] M. N. Barber, in *Phase Transitions and Critical Phenomena,* edited by C. Domb and J. L. Lebowitz (Academic, London, 1983), Vol. 8, p. 145.
[17] *Finite Size Scaling,* edited by J. L. Cardy (North-Holland, Amsterdam, 1988).
[18] P. A. Lee and T. V. Ramakrishnan, Rev. Mod. Phys. **57**, 287 (1985).
[19] J. E. Avron and L. Sadun, Phys. Rev. Lett. **62**, 3082 (1989); J. E. Avron, A. Raveh, and B. Zur, Rev. Mod. Phys. **60**, 873 (1988).
[20] R. Landauer, IBM Res. Dev. **1**, 223 (1957).
[21] J. L. Pichard, Thesis, Université de Paris–Sud, Orsay, 1984; N. Zanon and J. L. Pichard, J. Phys. (Paris) **49**, 907 (1988).
[22] R. M. Redheffer, J. Math. Phys. **41**, 1 (1962).
[23] Y. Avishai and Y. B. Band, Phys. Rev. Lett. **58**, 2251 (1987).
[24] H. Tsunetsugu, T. Fujiwara, K. Ueda, and T. Tokihiro, Phys. Rev. B **43**, 8879 (1991).
[25] J. T. Chayes, L. Chayes, D. S. Fisher, and T. Spencer, Commun. Math. Phys. **120**, 501 (1989).

[26]A. McKinnon and B. Kramer, Phys. Rev. Lett. **47**, 1546 (1981); Z. Phys. B **53**, 1 (1983); B. R. Bulka, B. Kramer, and A. McKinnon, *ibid.* **60**, 13 (1985); B. R. Bulka, M. Schreiber, and B. Kramer, *ibid.* **66**, 21 (1987); R. F. Loring and S. Mukamel, Phys. Rev. B **33**, 7708 (1986); D. E. Logan and P. G. Wolynes, J. Chem. Phys. **85**, 937 (1986); R. F. Loring, D. S. Franchi, and S. Mukamel, Phys. Rev. B **37**, 1874 (1988); R. F. Loring, M. Sparpaglione, and S. Mukamel, J. Chem. Phys. **86**, 2249 (1987).

[27]B. Altshuler, Pis'ma Zh. Eksp. Teor. Fiz. **41**, 530 (1985) [JETP Lett. **41**, 648 (1985)].

[28]E. Medina, M. Kardar, Y. Shapir, and Xiang Rong Wang, Phys. Rev. Lett. **62**, 941 (1989).

[29]K. M. Slevin and J. B. Pendry, J. Phys. Condens. Matter **2**, 2821 (1990); Phys. Rev. B **41**, 10 240 (1990).

[30]J. L. Pichard, M. Sanquer, K. Slevin, and P. Debray, Phys. Rev. Lett. **65**, 1812 (1990).

[31]J. P. Bouchaud (unpublished).

[32]I. M. Lifshitz, Adv. Phys. **13**, 483 (1964).